

**Probing neutron skin with free spectator nucleons
in ultracentral relativistic heavy-ion collisions**

Jun Xu (徐骏)

Tongji University

Main collaborators: Lu-Meng Liu (刘鹿蒙)(UCAS)

Jiangyong Jia (贾江涌)(Stony Brook)

Chun-Jian Zhang (张春健)(Stony Brook)

**Lu-Meng Liu, Chun-Jian Zhang, Jia Zhou, JX*, Jiangyong Jia*, and Guang-Xiong Peng,
Phys. Lett. B 834, 137441 (2022), arXiv: 2203.09924 [nucl-th]**

**Lu-Meng Liu, Chun-Jian Zhang, JX*, Jiangyong Jia*, and Guang-Xiong Peng,
Phys. Rev. C 106, 034913 (2022), arXiv: 2209.03106 [nucl-th]**

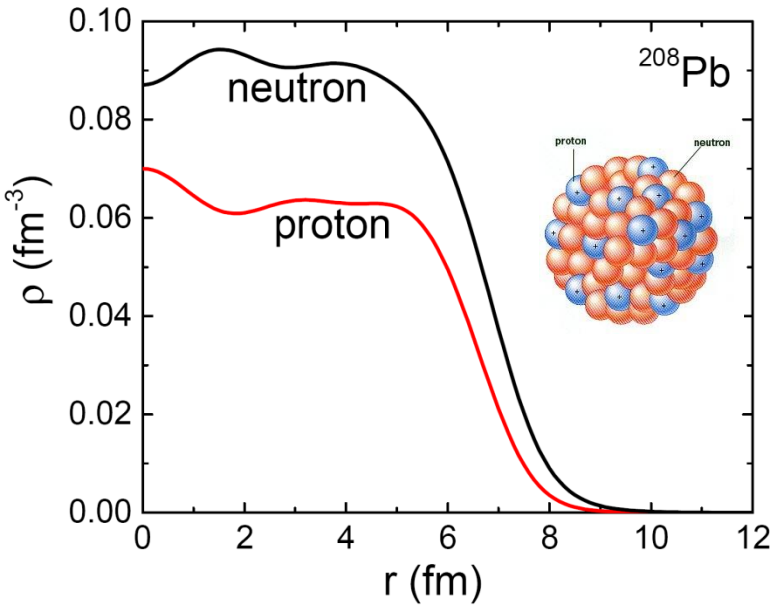
**Lu-Meng Liu, JX*, and Guang-Xiong Peng,
Nucl. Phys. Rev. 40, 2022095 (2023), arXiv: 2301.08251 [nucl-th]**

**Lu-Meng Liu, JX*, and Guang-Xiong Peng,
Phys. Lett. B 838, 137701 (2023), arXiv: 2301.07893 [nucl-th]**

Content

- **Background**
 - Neutron skin
 - Nuclear symmetry energy
- **Model setups**
 - Initial density distribution
 - Glauber model
 - Multifragmentation process
- **Results and discussions**
 - Probing $\Delta r_{np} \sim L$
 - Probing $\Delta r_{np}(\theta) \sim W_0$
- **Summary and outlook**

Neutron skin and E_{sym}



Neutron-Skin Thickness:

$$\Delta r_{\text{np}} = \sqrt{\langle r_n^2 \rangle} - \sqrt{\langle r_p^2 \rangle} \quad (\text{fm})$$

For ^{208}Pb :

$\Delta r_{\text{np}} = 0.211^{+0.054}_{-0.063}$ fm from proton scattering

$\Delta r_{\text{np}} = 0.16 \pm 0.07$ fm from pion scattering

$\Delta r_{\text{np}} = 0.18 \pm 0.04(\text{expt.}) \pm 0.05(\text{theor.})$ fm from \bar{p} annihilation

$\Delta r_{\text{np}} = 0.15 \pm 0.03(\text{stat.})^{+0.01}_{-0.03}(\text{sys.})$ fm from coherent pion photoproduction

$\Delta r_{\text{np}} = 0.283 \pm 0.071$ fm from parity-violating electron scatterings

Energy per nucleon
in asymmetric matter

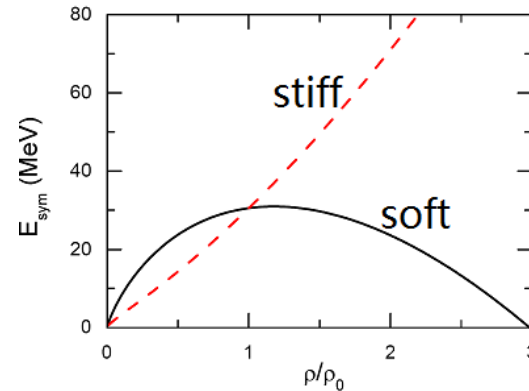
Symmetry energy

$$E(\rho, \delta) \approx E_0(\rho) + E_{\text{sym}}(\rho) \delta^2$$

Energy per nucleon
in symmetric matter

$$\rho = \rho_n + \rho_p$$

$$\delta = (\rho_n - \rho_p) / \rho$$



Expansion around saturation density ρ_0

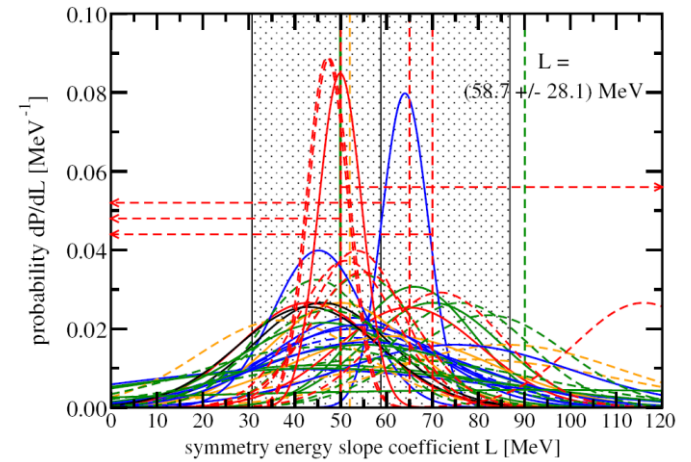
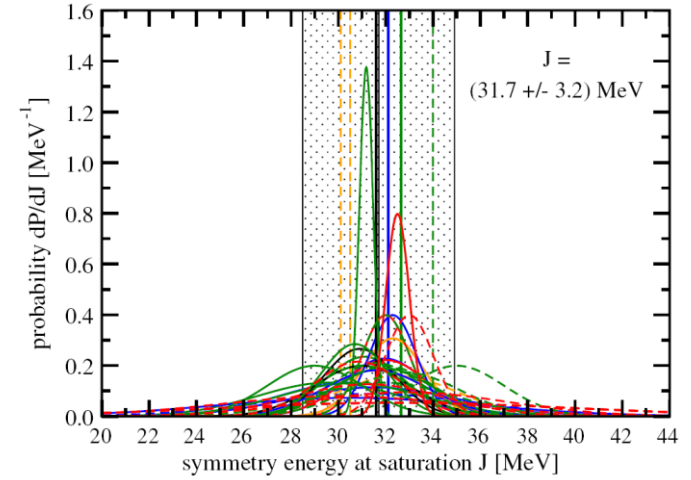
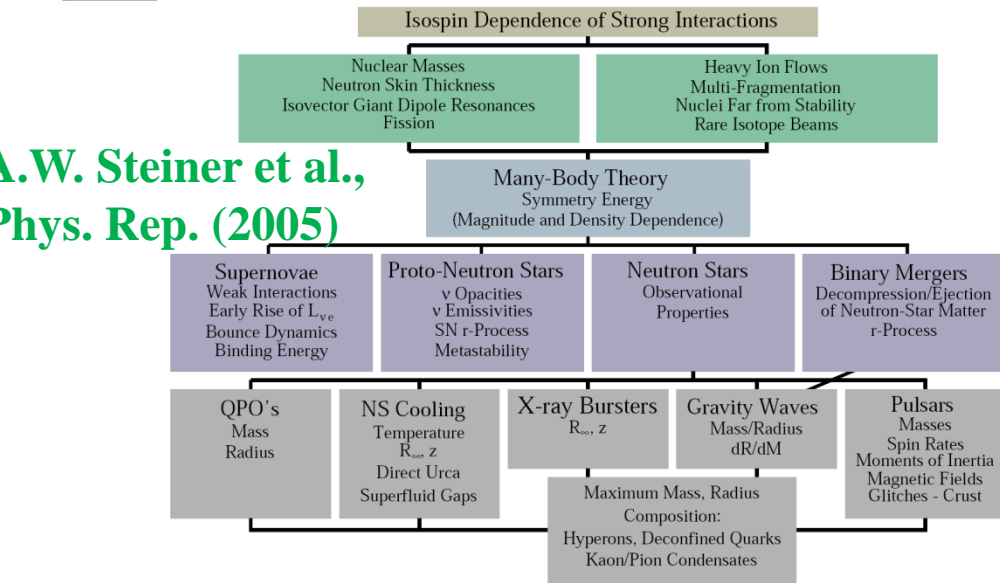
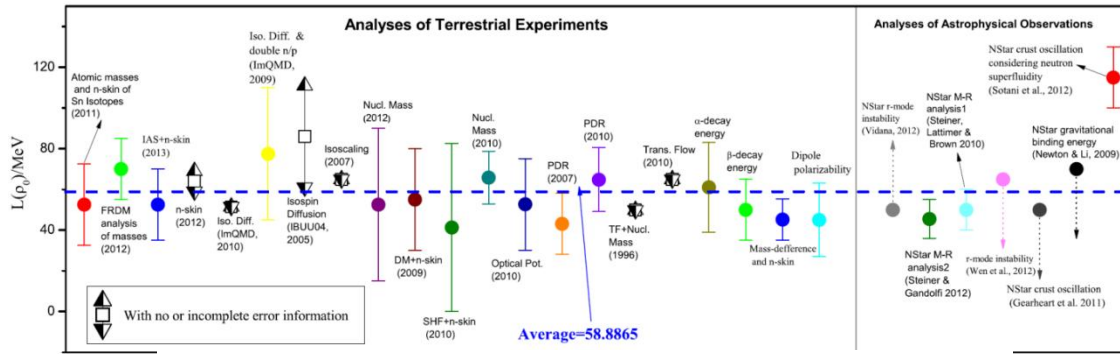
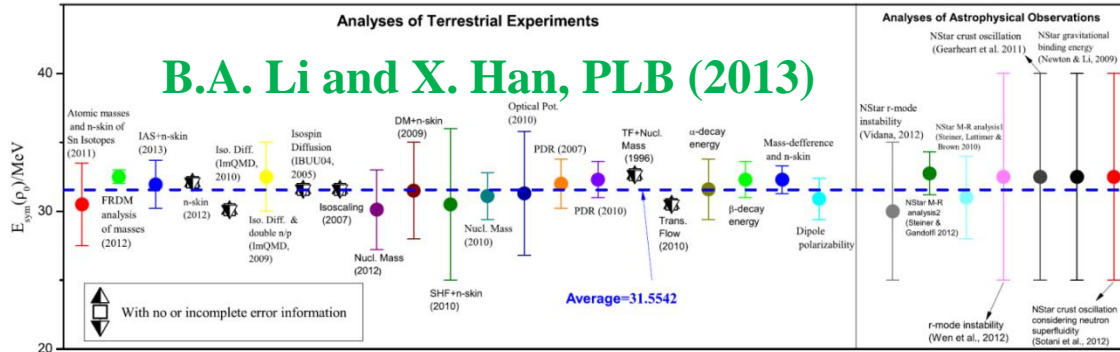
$$E_{\text{sym}}(\rho) = E_{\text{sym}}(\rho_0) + L\chi + \dots$$

$$\chi = \frac{\rho - \rho_0}{3\rho_0}$$

Slope parameter

$$L = 3\rho_0 \left[\frac{\partial E_{\text{sym}}(\rho)}{\partial \rho} \right]_{\rho=\rho_0}$$

Various constraints on $E_{\text{sym}}(\rho_0)$ and $L(\rho_0)$

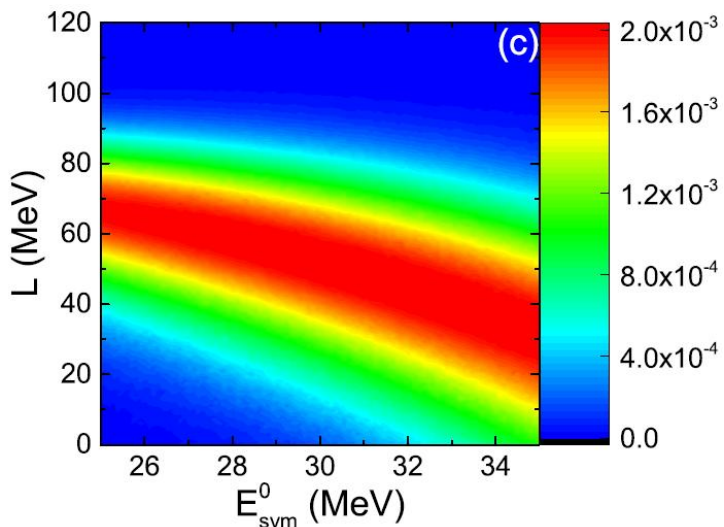


M. Oertel et al., RMP (2017)

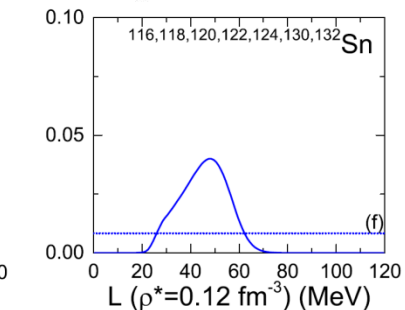
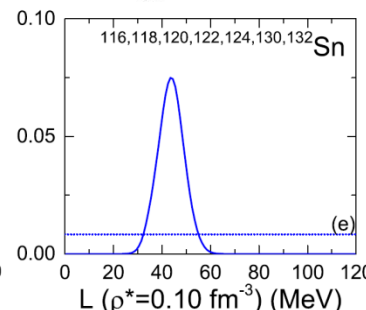
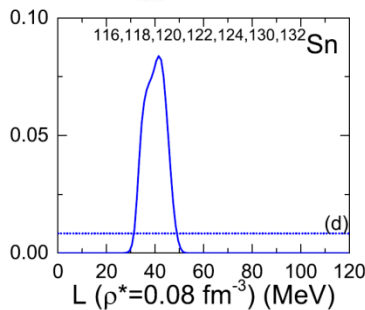
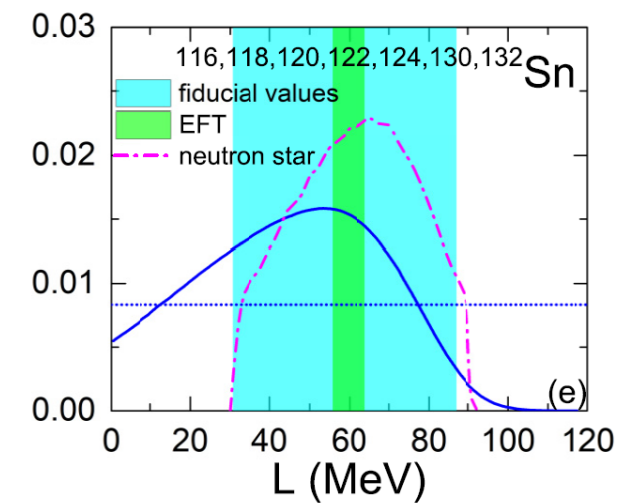
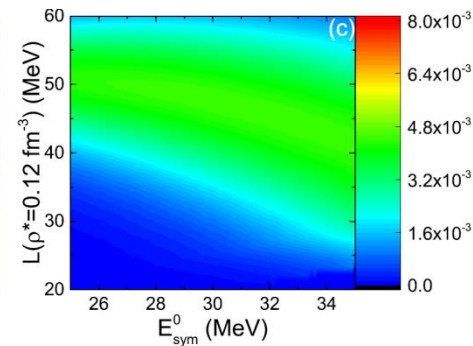
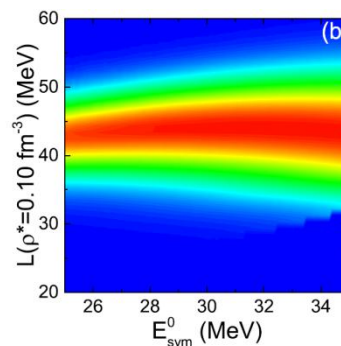
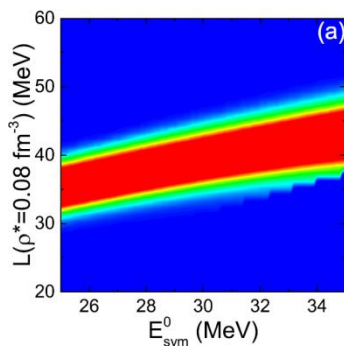
Symmetry energy PACS: 21.65.Ef

More reliable probes are still needed

Constraint on E_{sym} from Δr_{np}

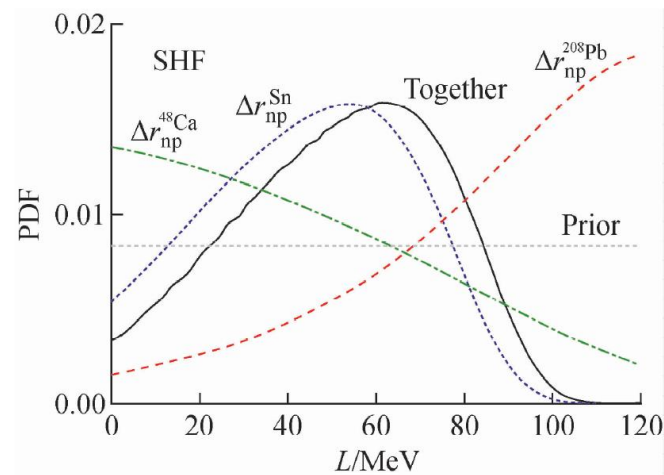


Δr_{np} dominated by $L(0.10)$ $L(\rho^*) = 3\rho^*(dE_{\text{sym}}/d\rho)_{\rho^*}$



^{208}Pb : PREXII
 Sn : p-Sn scatterings
 ^{48}Ca : CREX

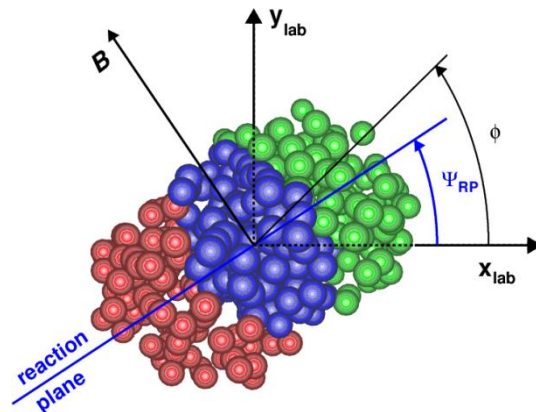
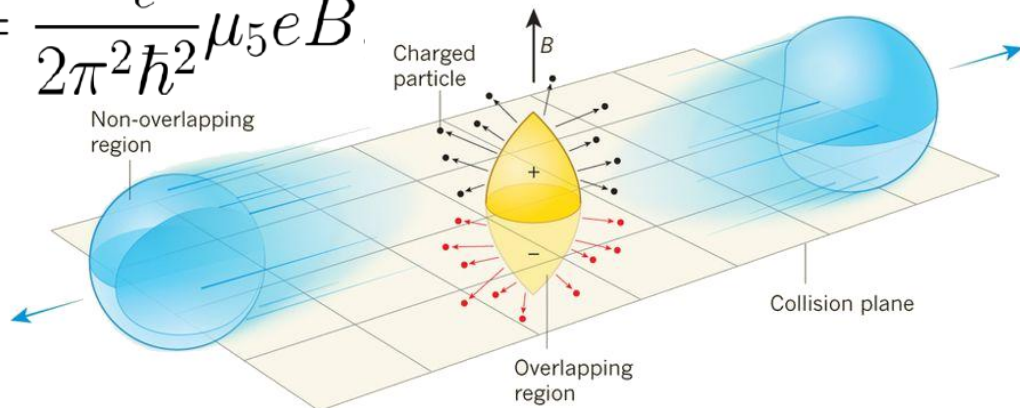
JX, arXiv:
 2301.07884 [nucl-th]



JX, W.J. Xie, and B.A. Li,
 PRC (2020)

CME and isobaric collisions

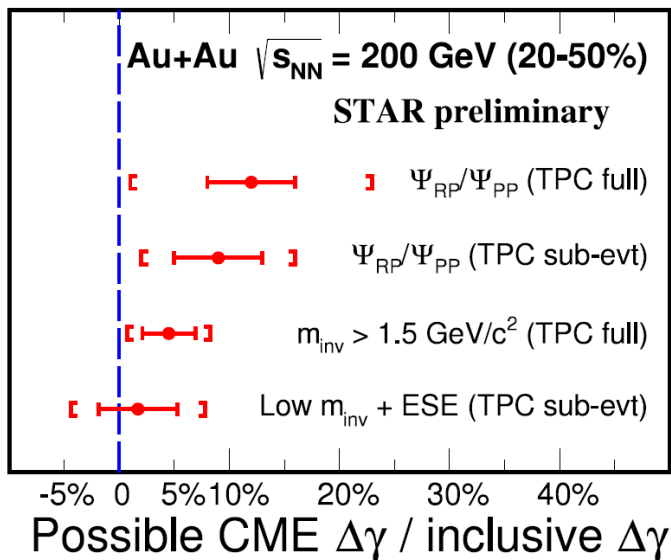
$$\vec{J} = \frac{N_c}{2\pi^2 \hbar^2} \mu_5 e \vec{B}$$



$$\gamma_{\alpha\beta} = \langle \cos(\phi_\alpha + \phi_\beta - 2\Psi_2) \rangle$$

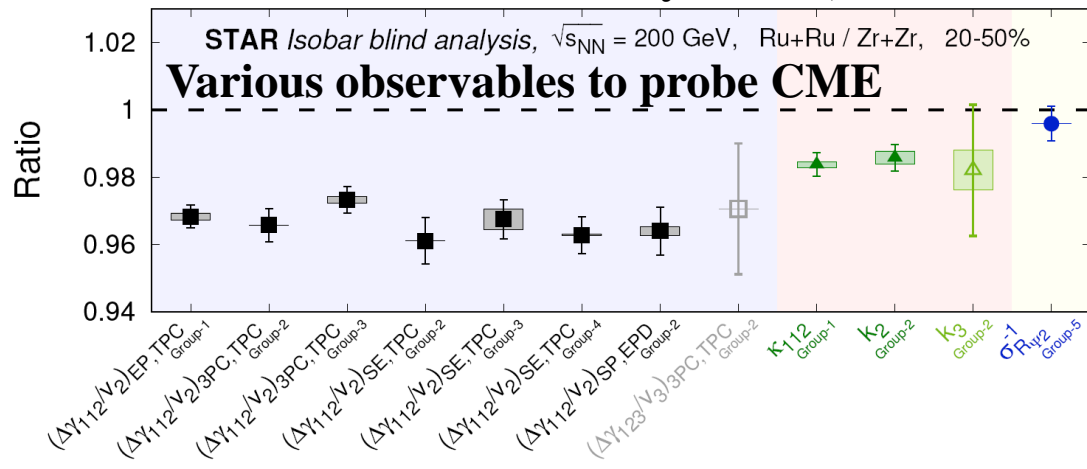
S. A. Voloshin, PRC (2004)

Significant background contribution



J. Zhao and F.Q. Wang, PPNP (2019)

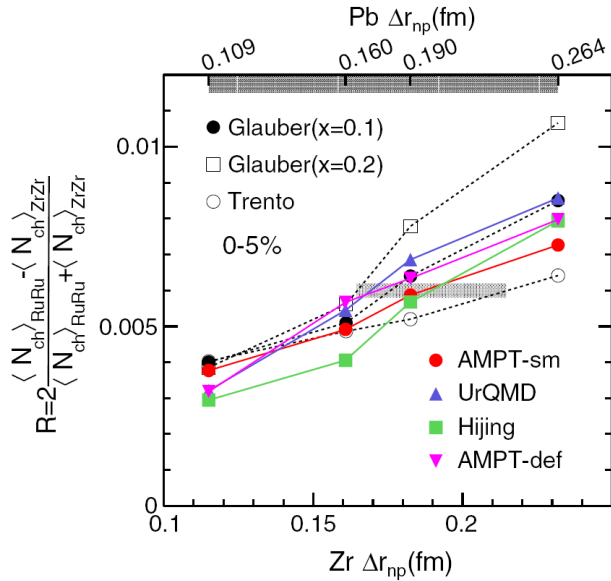
Isobaric collisions: similar bulk dynamics, different B



STAR, PRC (2022)

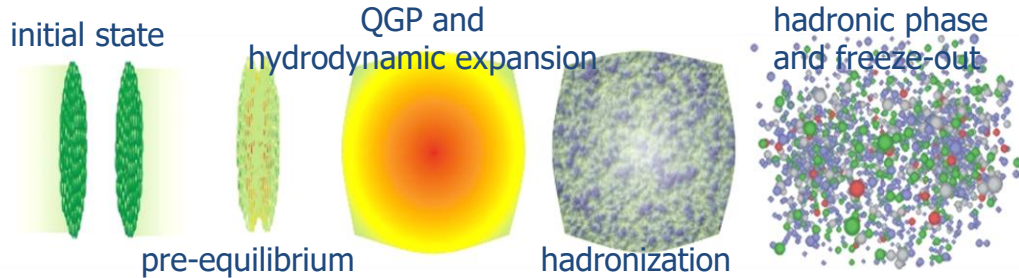
Isobaric collisions to probe neutron skin

Charged-particle multiplicity



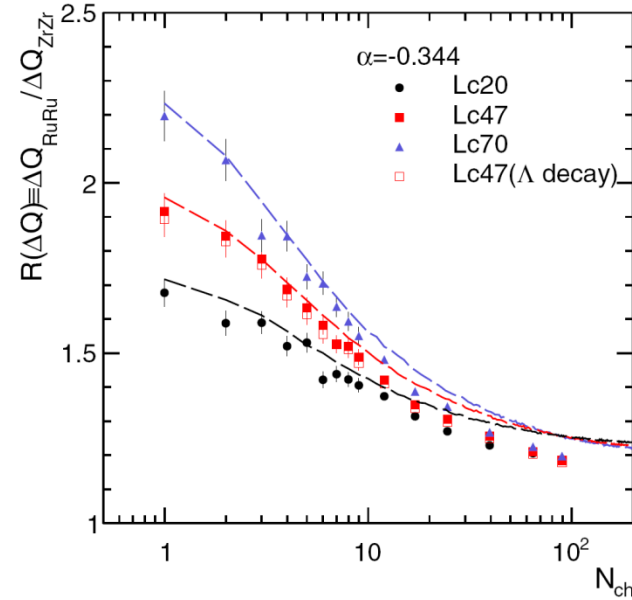
H.L. Li et al., PRL (2020)

probe the density distribution of colliding nuclei



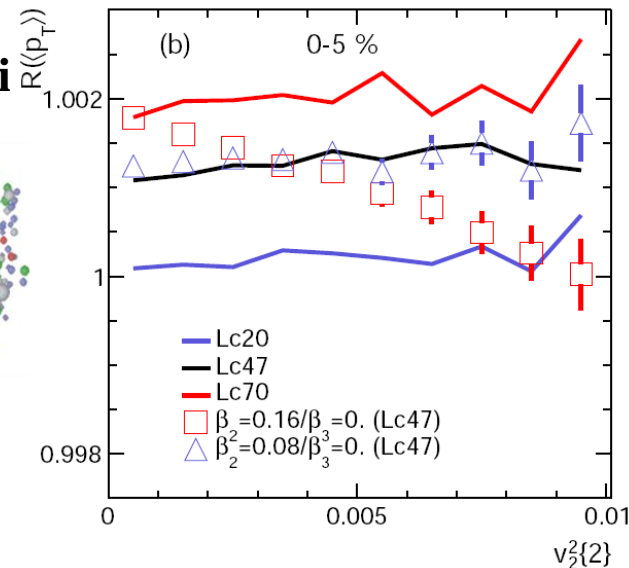
Observables at midrapidity suffer from complicated dynamics and model dependence

Net-charge multiplicity



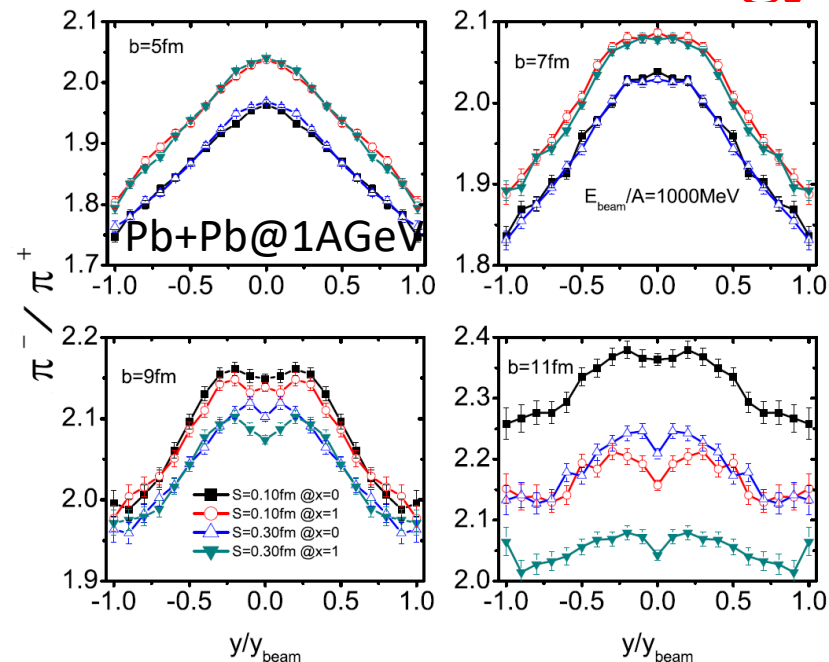
H.J. Xu et al., PRC (2020)

Average transverse momentum

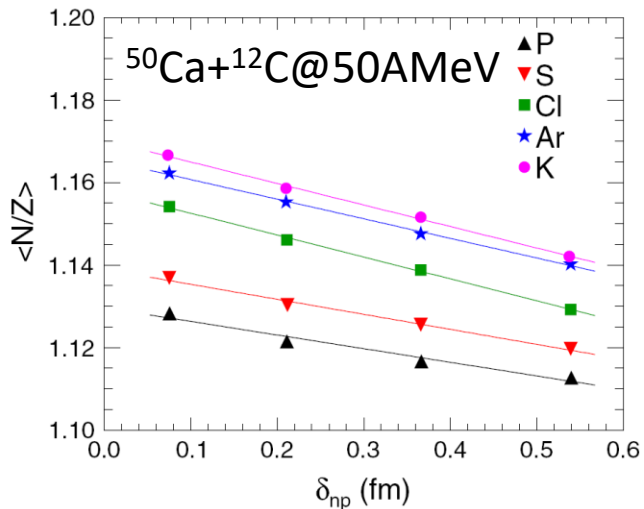


H.J. Xu et al., arXiv: 2111.14812 [nucl-th]

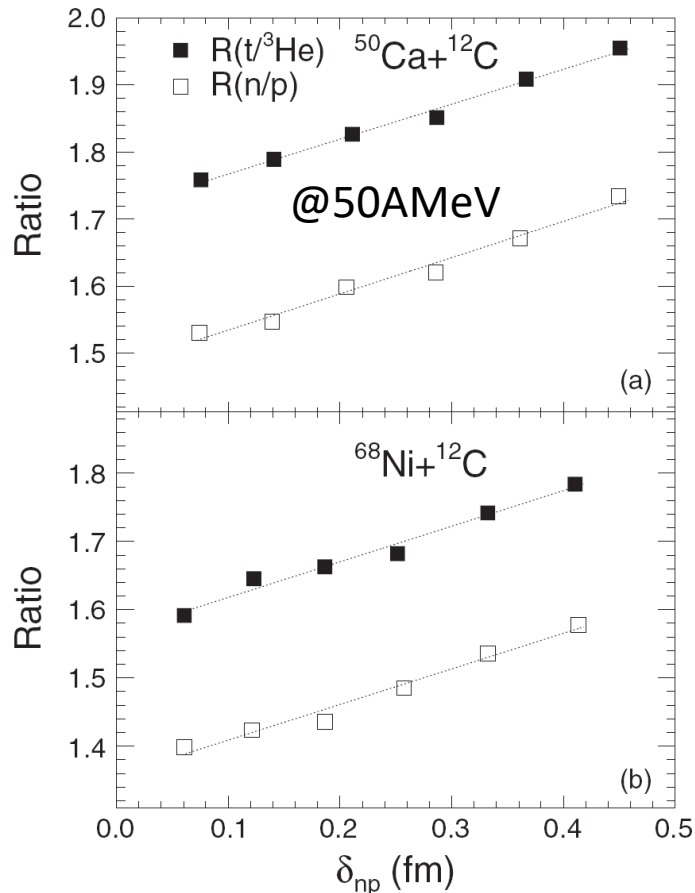
Intermediate-energy HIC to probe neutron skin



G.F. Wei et al., PRC (2014)



Z.T. Dai et al., PRC (2015)

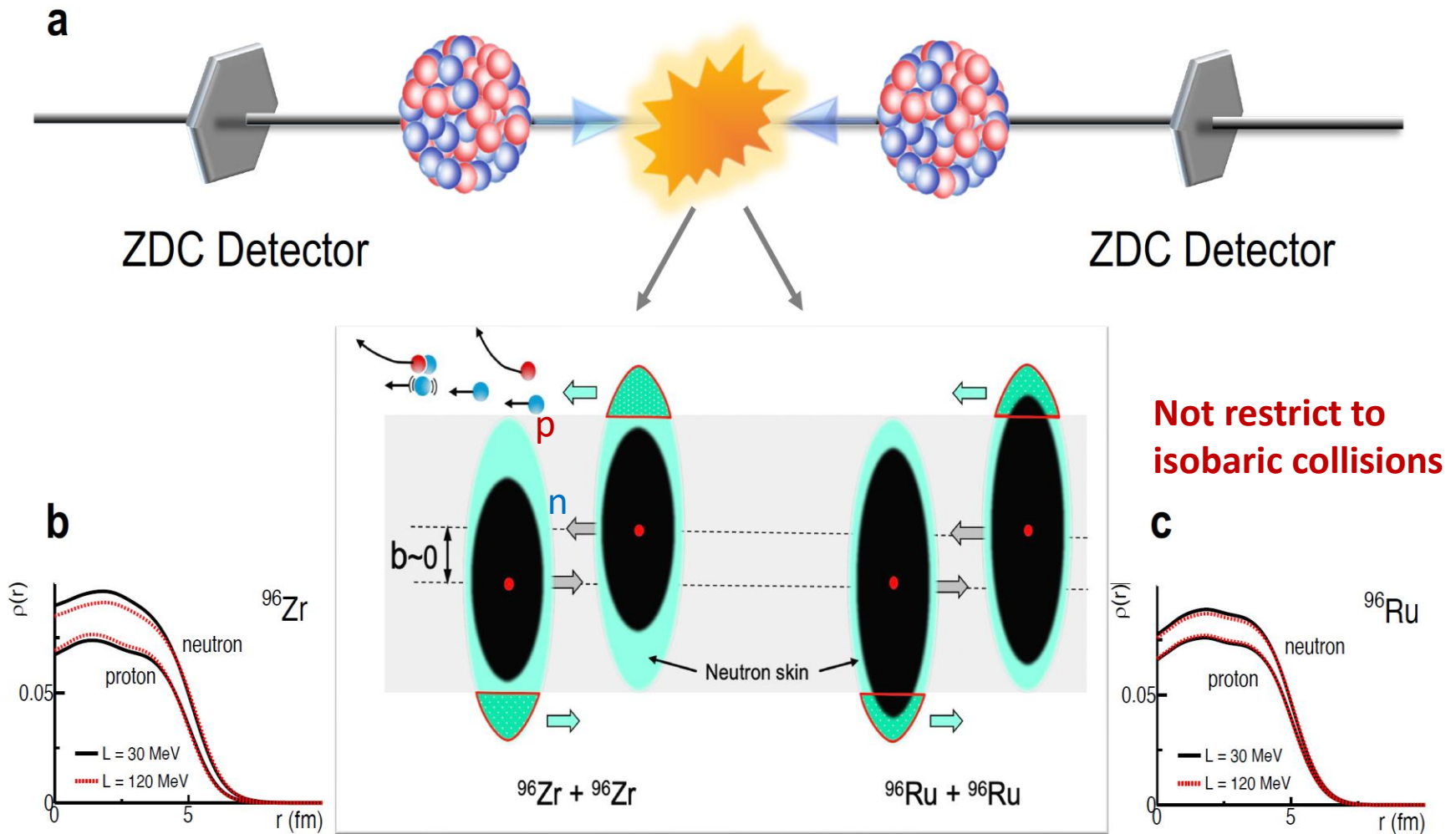


Z.T. Dai et al., PRC (2014)

Suffer from:

- 1) Model dependence
- 2) Interaction between spectator and participant
- 3) Uncertainties of clusterization/multifragmentation

Basic idea of our studies



Advantages:

- 1) Spectator matter has almost no interaction with participant matter
- 2) UCC region, free from uncertainties of clusterization/multifragmentation

Model setup: initial density distribution

Skyrme-Hartree-Fock (SHF) model:

$$\begin{aligned}
 v(\vec{r}_1, \vec{r}_2) = & t_0(1 + x_0 P_\sigma) \delta(\vec{r}) \\
 & + \frac{1}{2} t_1(1 + x_1 P_\sigma) [\vec{k}'^2 \delta(\vec{r}) + \delta(\vec{r}) \vec{k}^2] \\
 & + t_2(1 + x_2 P_\sigma) \vec{k}' \cdot \delta(\vec{r}) \vec{k} \\
 & + \frac{1}{6} t_3(1 + x_3 P_\sigma) \rho^\alpha(\vec{R}) \delta(\vec{r}) \\
 & + iW_0(\vec{\sigma}_1 + \vec{\sigma}_2) [\vec{k}' \times \delta(\vec{r}) \vec{k}].
 \end{aligned}$$

Hartree-Fock method:

$$\begin{aligned}
 E = & \sum_i \langle i | \frac{p^2}{2m} | i \rangle + \frac{1}{2} \sum_{ij} \langle ij | \bar{v}_{12} | ij \rangle \\
 \frac{\delta}{\delta \phi_i} \left(E - \sum_i e_i \int |\phi_i(\vec{r})|^2 d^3r \right) = & 0 \\
 \left[-\vec{\nabla} \cdot \frac{\hbar^2}{2m_q^*(\vec{r})} \vec{\nabla} + U_q(\vec{r}) + \vec{W}_q(\vec{r}) \cdot (-i)(\vec{\nabla} \times \vec{\sigma}) \right] \phi_i = & e_i \phi_i
 \end{aligned}$$

Particle density

$$\rho_q(\vec{r}) = \sum_{i, \sigma} |\phi_i(\vec{r}, \sigma, q)|^2$$

Reproduce E_b and R_c within 1.5%

Quantity	MSL0	Quantity	MSL0
t_0 (MeV fm ⁵)	-2118.06	ρ_0 (fm ⁻³)	0.16
t_1 (MeV fm ⁵)	395.196	E_0 (MeV)	-16.0
t_2 (MeV fm ⁵)	-63.953 1	K_0 (MeV)	230.0
t_3 (MeV fm ^{3+3\sigma})	128 57.7	$m_{s,0}^*/m$	0.80
x_0	-0.070 949 6	$m_{s,0}^*/m$	0.70
x_1	-0.332 282	$E_{\text{sym}}(\rho_0)$ (MeV)	30.0
x_2	1.358 30	L (MeV)	60.0
x_3	-0.228 181	G_S (MeV fm ⁵)	132.0
σ	0.235 879	G_V (MeV fm ⁵)	5.0
W_0 (MeV fm ⁵)	133.3	$G'_0(\rho_0)$	0.42

L.W. Chen,
C.M. Ko,
B.A. Li, and JX
PRC (2010)

Pairing interaction

$$V_{\text{pair}}^{(n,p)} = V_0^{(n,p)} \left(1 - \frac{1}{2} \frac{\rho(\vec{r})}{\rho_0} \right) \delta(\vec{r}_1 - \vec{r}_2)$$

Hartree-Fock-Bogoliubov method:

$$\begin{aligned}
 \int d^3r' \sum_{\sigma'} \begin{pmatrix} h(\mathbf{r}\sigma, \mathbf{r}'\sigma') & \tilde{h}(\mathbf{r}\sigma, \mathbf{r}'\sigma') \\ \tilde{h}(\mathbf{r}\sigma, \mathbf{r}'\sigma') & -h(\mathbf{r}\sigma, \mathbf{r}'\sigma') \end{pmatrix} \begin{pmatrix} \varphi_1(E, \mathbf{r}'\sigma') \\ \varphi_2(E, \mathbf{r}'\sigma') \end{pmatrix} \\
 = \begin{pmatrix} E + \lambda & 0 \\ 0 & E - \lambda \end{pmatrix} \begin{pmatrix} \varphi_1(E, \mathbf{r}\sigma) \\ \varphi_2(E, \mathbf{r}\sigma) \end{pmatrix}
 \end{aligned}$$

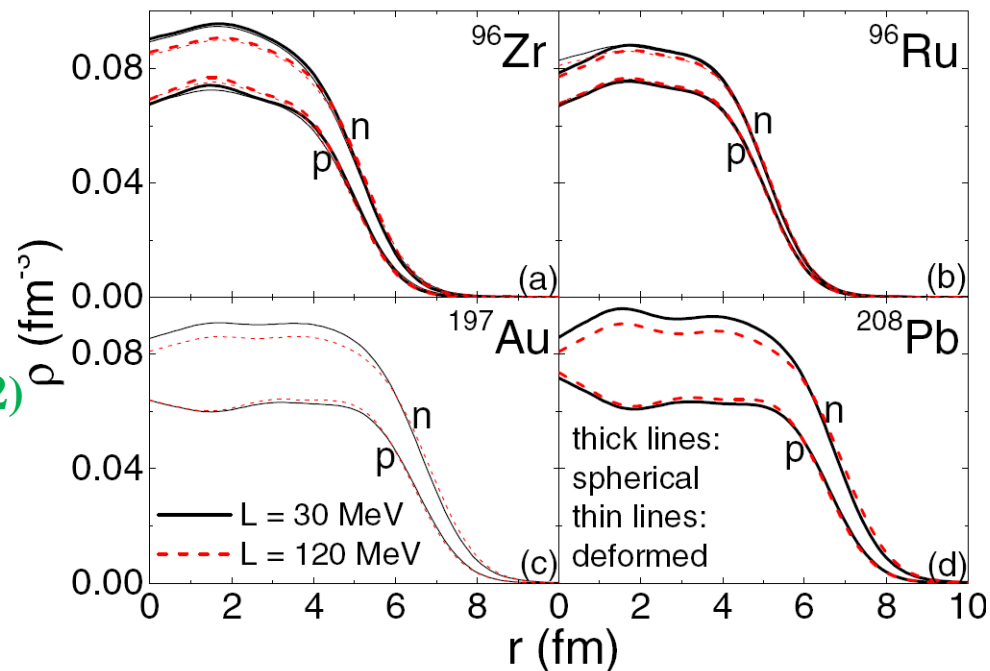
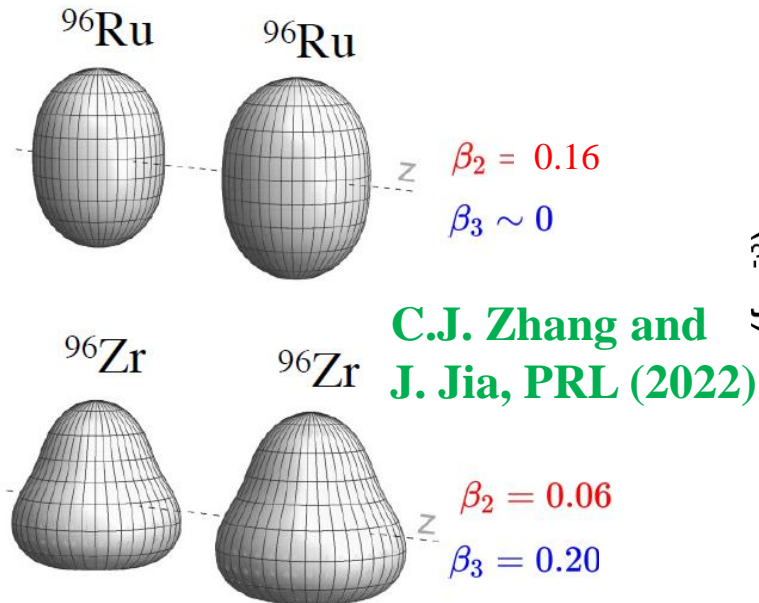
Particle density

$$\rho(r) = \sum_i \varphi_2(E_i, r)^2 \quad \tilde{\rho}(r) = - \sum_i \varphi_1(E_i, r) \varphi_2(E_i, r)$$

Pairing density

M.V. Stoitsov et al., CPC (2013)

Model setup: initial density distribution



Multipole moments

$$Q_{\lambda,\tau} = \int \rho_{\tau}(\vec{r}) r^{\lambda} Y_{\lambda 0}(\theta) d^3 r$$

Deformation parameters

$$\beta_{\lambda,\tau} = \frac{4\pi Q_{\lambda,\tau}}{3N_{\tau}R^{\lambda}}$$

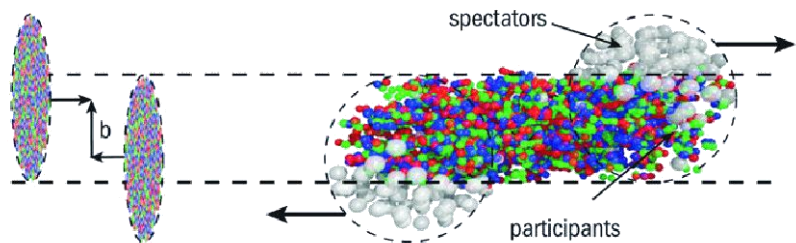
TABLE II. Neutron-skin thicknesses Δr_{np} and deformation parameters β_2 and β_3 for different nuclei using different slope parameters L of the symmetry energy from SHFB calculations.

Nucleus	β_2, β_3	Δr_{np} (fm)	
		$L = 30$ MeV	$L = 120$ MeV
^{96}Zr	0, 0	0.147	0.231
	0.06, 0.2 [43]	0.145	0.227
^{96}Ru	0, 0	0.028	0.061
	0.16, 0 [43]	0.026	0.058
^{197}Au	-0.15, 0 [44,45]	0.127	0.243
^{208}Pb	0, 0	0.149	0.281

Constrained SHFB calculation with fixed Q_{λ} (β_{λ})

Model setup: Glauber model

Schematic Monte-Carlo Glauber model



Numbers of sources

$$N_s = (1 - x) \frac{N_{\text{part}}}{2} + x N_{\text{coll}}$$

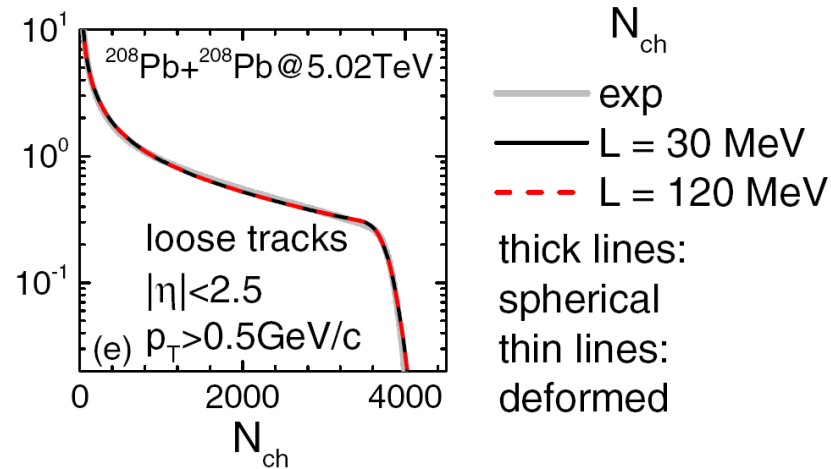
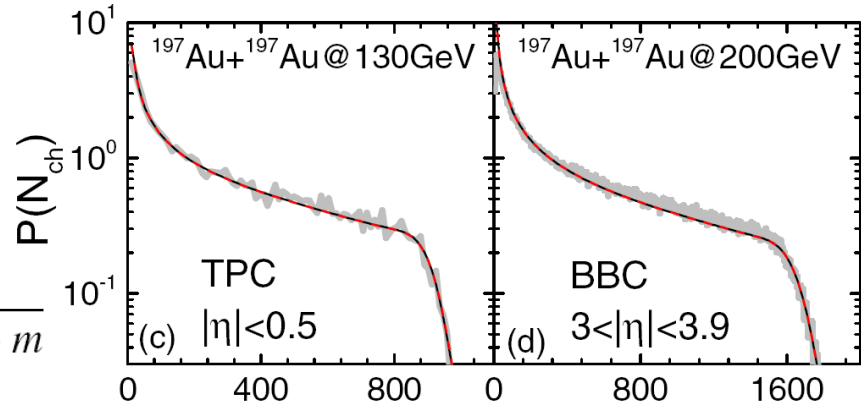
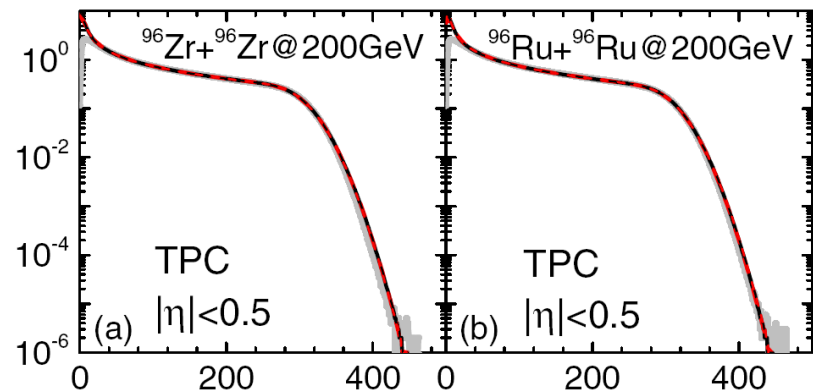
Particle production n from each source

$$p_{\text{nbnd}}(n; m, p) = \frac{(n + m - 1)!}{(m - 1)! n!} p^n (1 - p)^m$$

$$p = \frac{\bar{n}}{\bar{n} + m}$$

$\sqrt{s_{NN}}$	130 GeV	200 GeV	5.02 TeV
σ_{NN}	40 mb	42 mb	68 mb

	$\sqrt{s_{NN}}$	x	\bar{n}	m
$^{96}\text{Zr} + ^{96}\text{Zr}$	200 GeV	0.12	2.3	2.0
$^{96}\text{Ru} + ^{96}\text{Ru}$	200 GeV	0.12	2.3	2.2
$^{197}\text{Au} + ^{197}\text{Au}$	130 GeV	0	4.8	4.6
$^{197}\text{Au} + ^{197}\text{Au}$	200 GeV	0.10	5.8	2.3
$^{208}\text{Pb} + ^{208}\text{Pb}$	5.02 TeV	0.09	10.3	3.2



Model setup: multifragmentation process

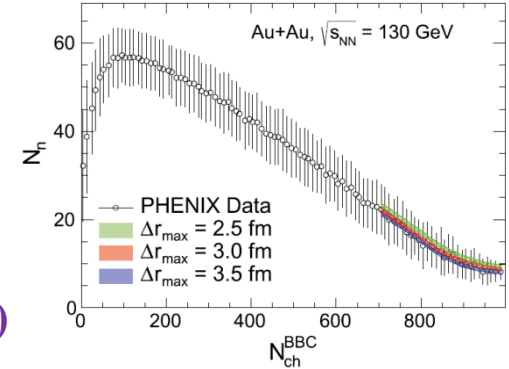
Dynamics of participant matter is neglected!

A. Formation of heavy ($A > 3$) clusters

MST

$\Delta r < 3$ fm (empirical nucleon interaction range)

$\Delta p < 300$ MeV/c (empirical Fermi momentum at ρ_0)



B. Heavy ($A > 3$) cluster deexcitation with GEMINI

1. Excitation energy

$$E = \frac{1}{N_{TP}} \sum_i \left(\sqrt{m^2 + p_i^2} - m \right)$$

Simplified
SHF EDF

$$+ \int d^3r \left[\frac{a}{2} \left(\frac{\rho}{\rho_0} \right)^2 + \frac{b}{\sigma+1} \left(\frac{\rho}{\rho_0} \right)^{\sigma+1} \right] + \int d^3r \left\{ \frac{G_S}{2} (\nabla \rho)^2 - \frac{G_V}{2} [\nabla(\rho_n - \rho_p)]^2 \right\}$$

$$+ \int d^3r E_{sym}^{pot} \left(\frac{\rho}{\rho_0} \right)^\gamma \frac{(\rho_n - \rho_p)^2}{\rho} + \frac{e^2}{2} \int d^3r d^3r' \frac{\rho_p(\vec{r}) \rho_p(\vec{r}')}{|\vec{r} - \vec{r}'|} - \frac{3e^2}{4} \int d^3r \left[\frac{3\rho_p}{\pi} \right]^{4/3} - E_{GS}$$

(test-particle method for parallel events
with similar collision configuration)

2. Angular momentum

$$\vec{L} = \sum_i \vec{r}_i \times \vec{p}_i$$

Free nucleons:

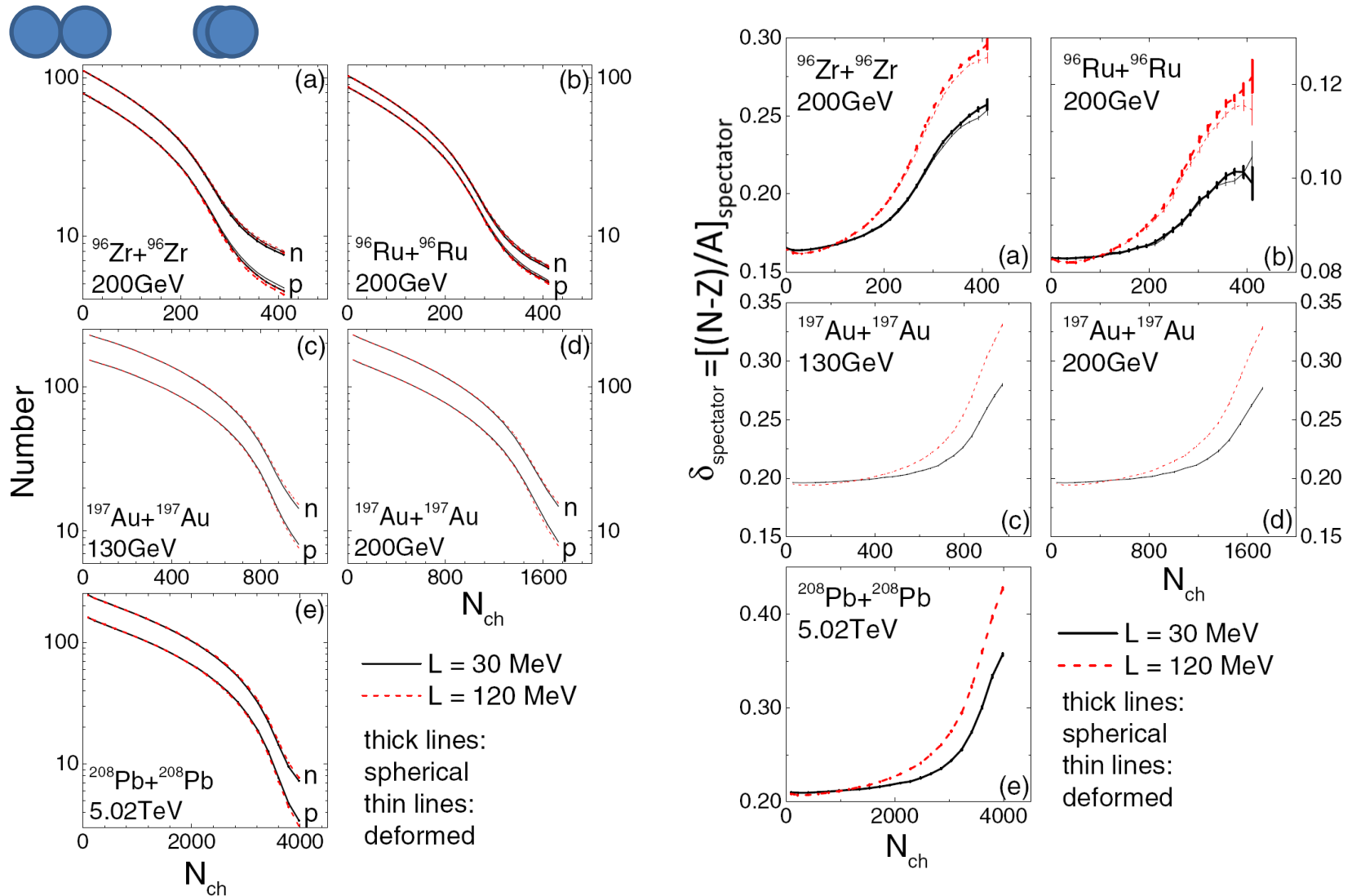
1) Direct production from A and residue from C

2) Deexcitation from B

C. Coalescence for light ($A=2,3$) clusters

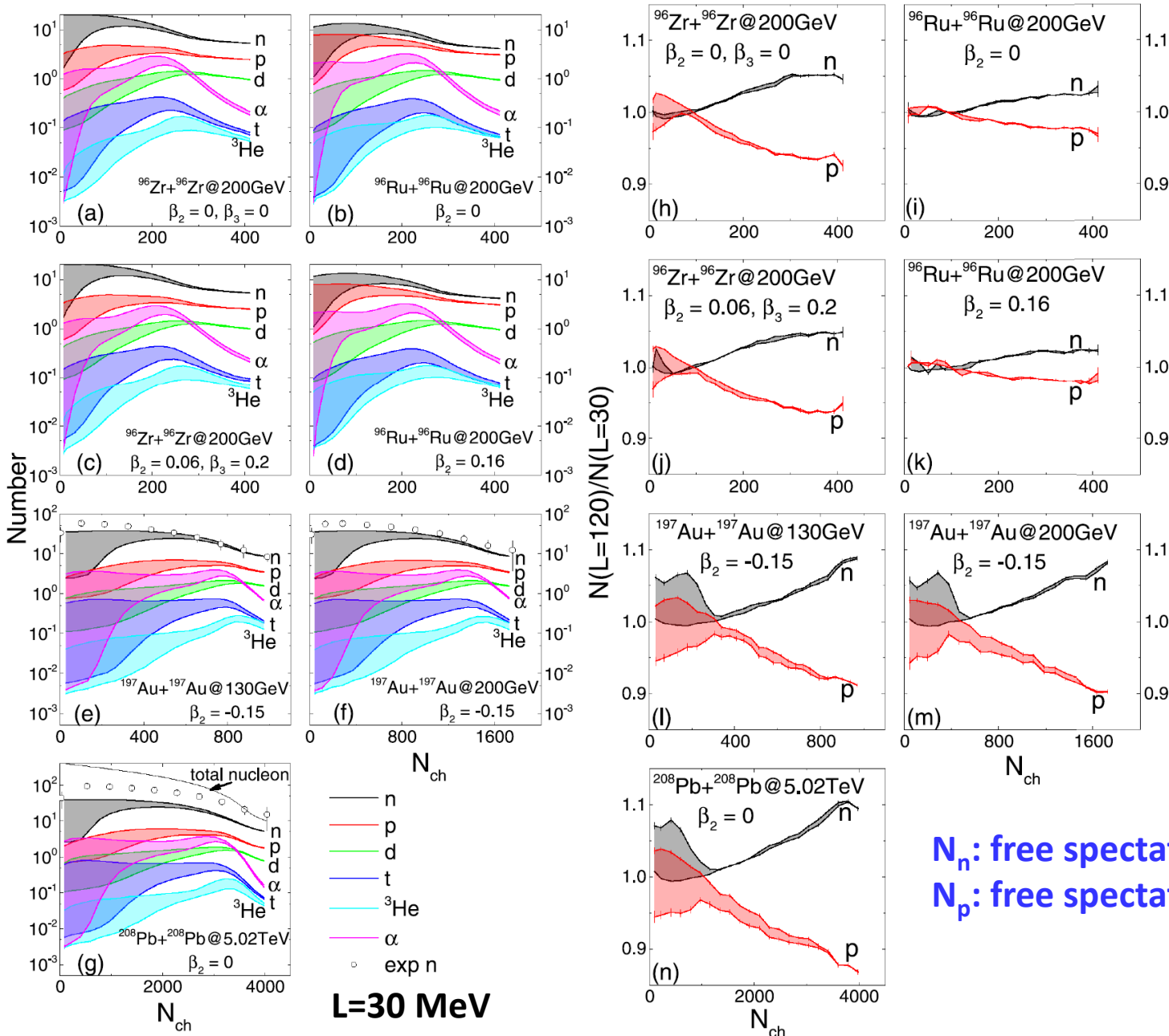
$$f_d = 8g_d \exp \left(-\frac{\rho^2}{\sigma_d^2} - p_\rho^2 \sigma_d^2 \right) \quad f_{t/{}^3\text{He}} = 8^2 g_{t/{}^3\text{He}} \exp \left[-\left(\frac{\rho^2 + \lambda^2}{\sigma_{t/{}^3\text{He}}^2} \right) - (p_\rho^2 + p_\lambda^2) \sigma_{t/{}^3\text{He}}^2 \right]$$

Results and discussions: spectator matter



- More neutron-rich spectator matter in more neutron-rich system
- More neutron-rich spectator matter in more central collisions (large N_{ch})
- More neutron-rich spectator matter with a larger L or a thicker neutron skin Δr_{np}

Results and discussions: spectator particle yield

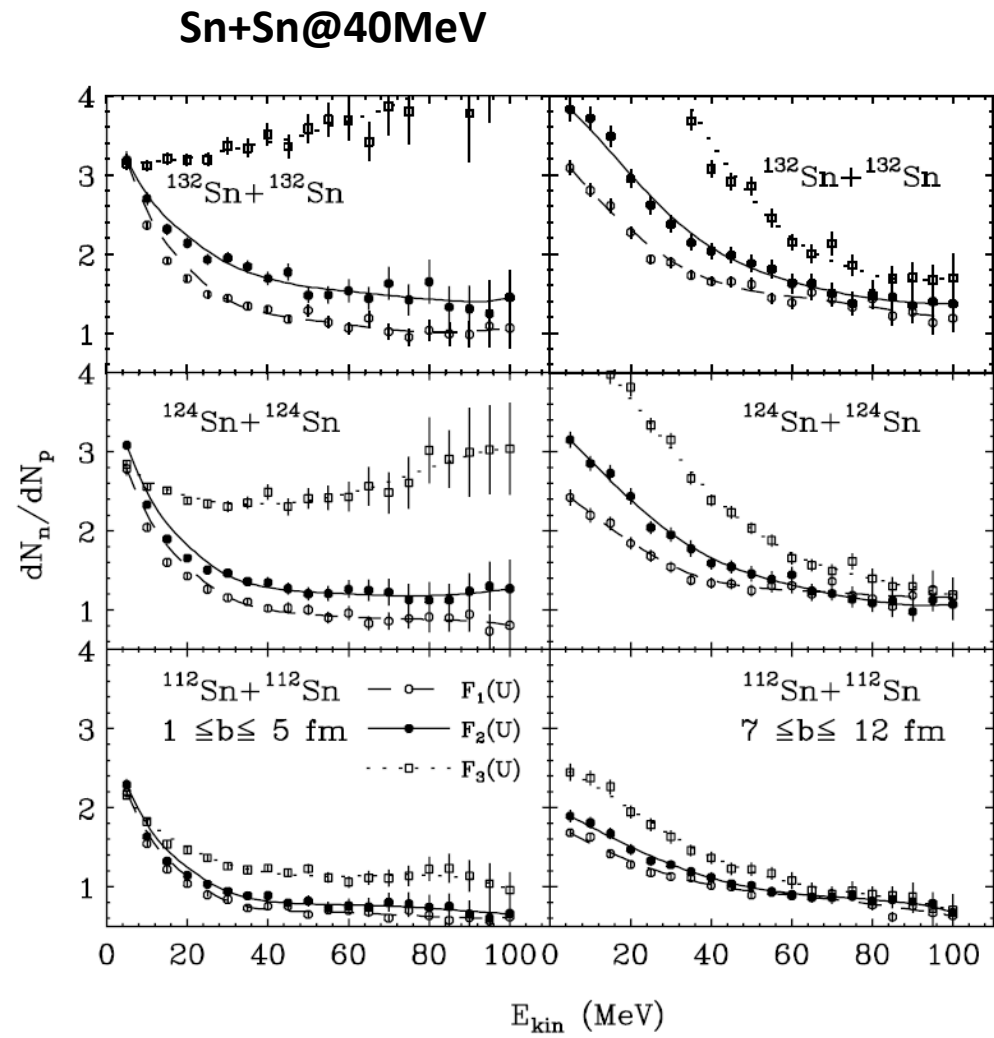
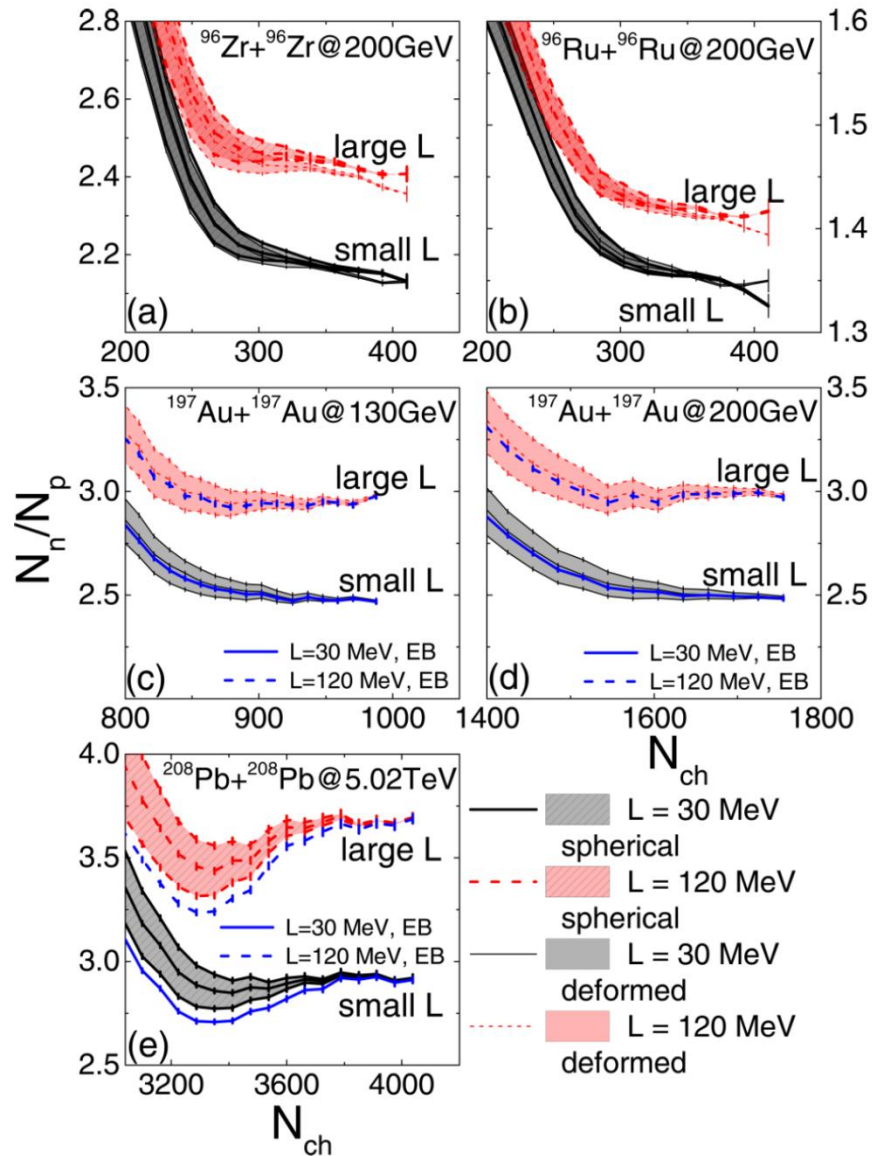


Band:
 $E/A \pm 1 \text{ MeV}$

- **Non monotonic dependence on N_{ch}**
- **Difference between N_n and N_p large at UCC, increasing with L or Δr_{np} , with small band**
- **Underestimate N_n at high energies (background?)**

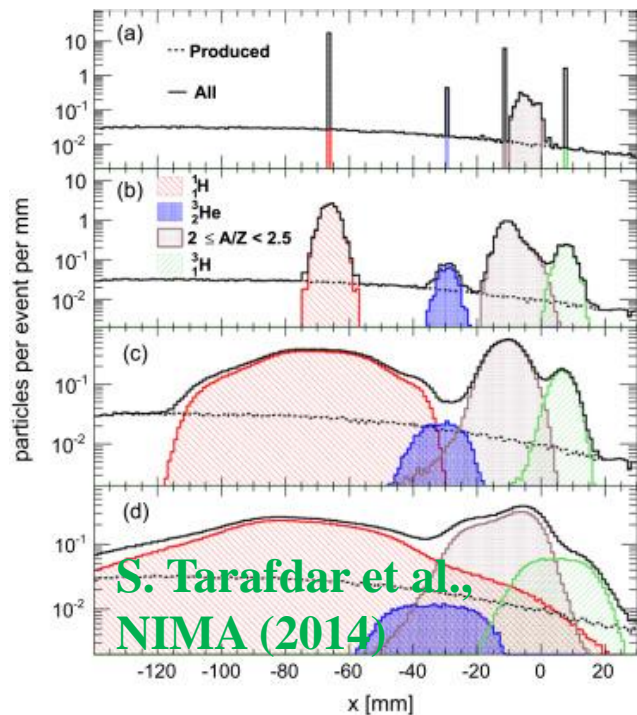
N_n : free spectator neutron number
 N_p : free spectator proton number

Results and discussions: probing L or Δr_{np}

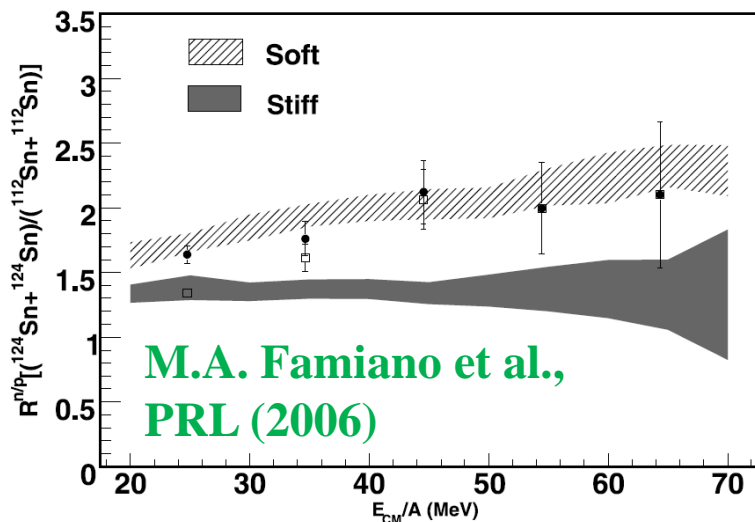


B.A. Li, C.M. Ko, and Z.Z. Ren, PRL (1997)

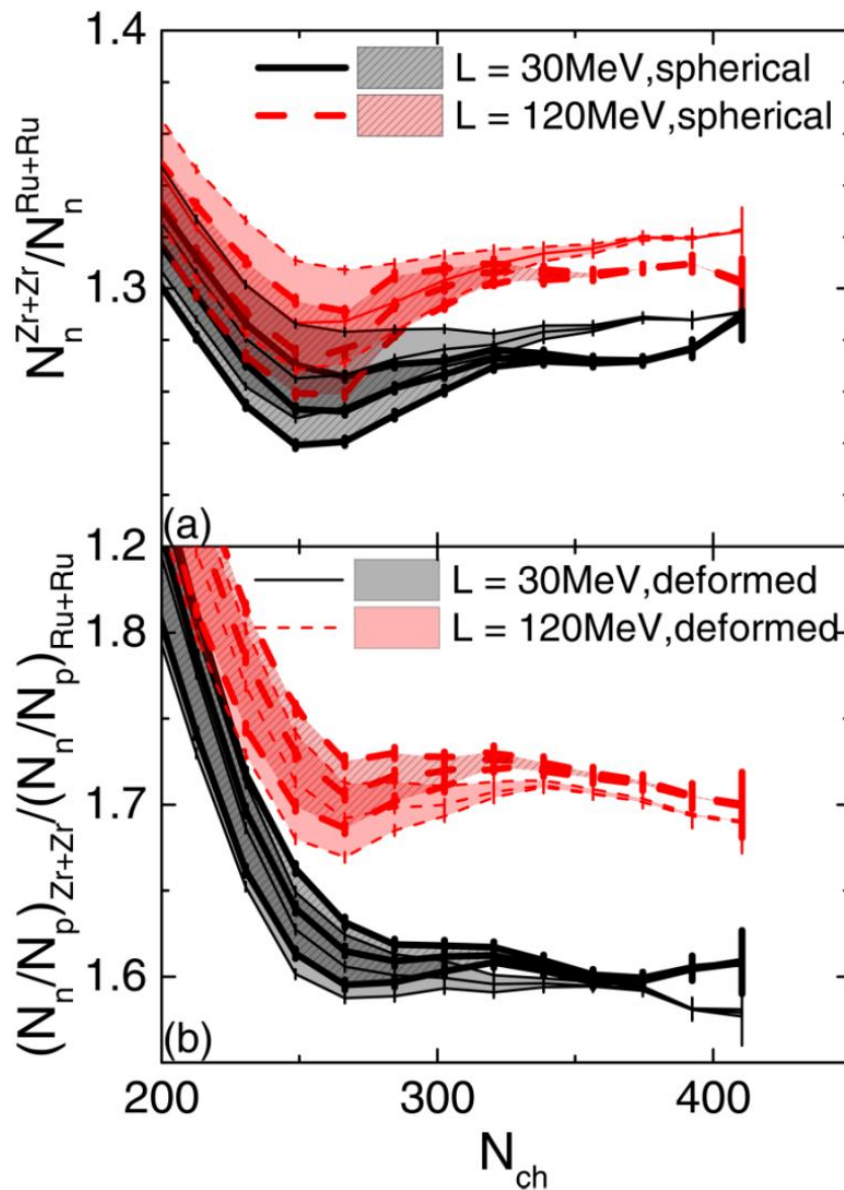
Results and discussions: probing L or Δr_{np}



S. Tarafdar et al.,
NIMA (2014)

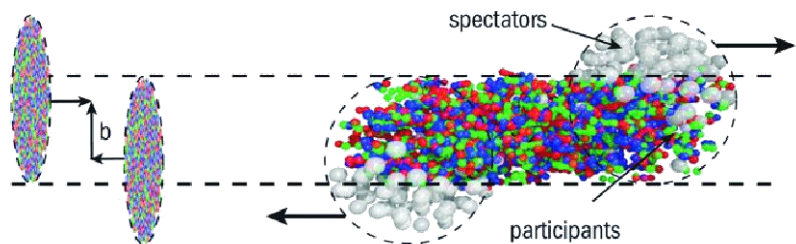


M.A. Famiano et al.,
PRL (2006)



Results and discussions: effects from EB field

Spectator protons pushed by EB field generated by another colliding nucleus



Lienard-Wiechert formulas

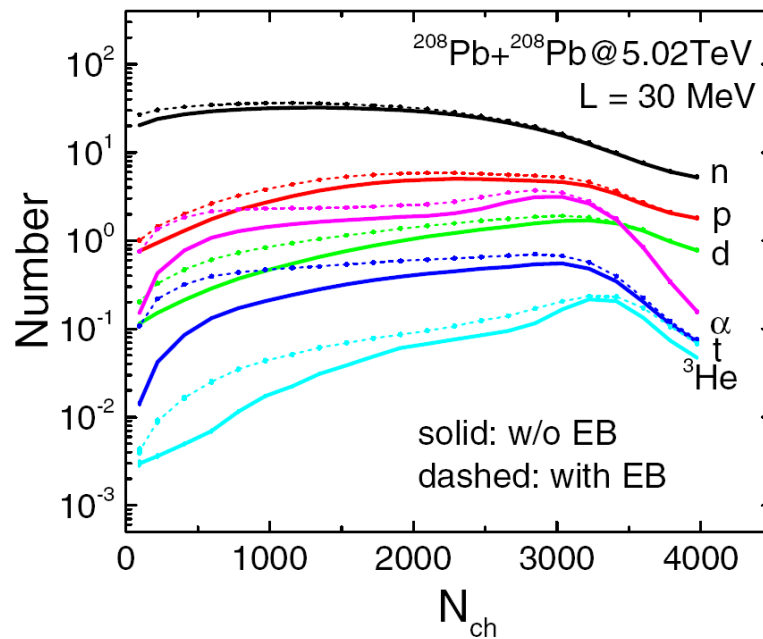
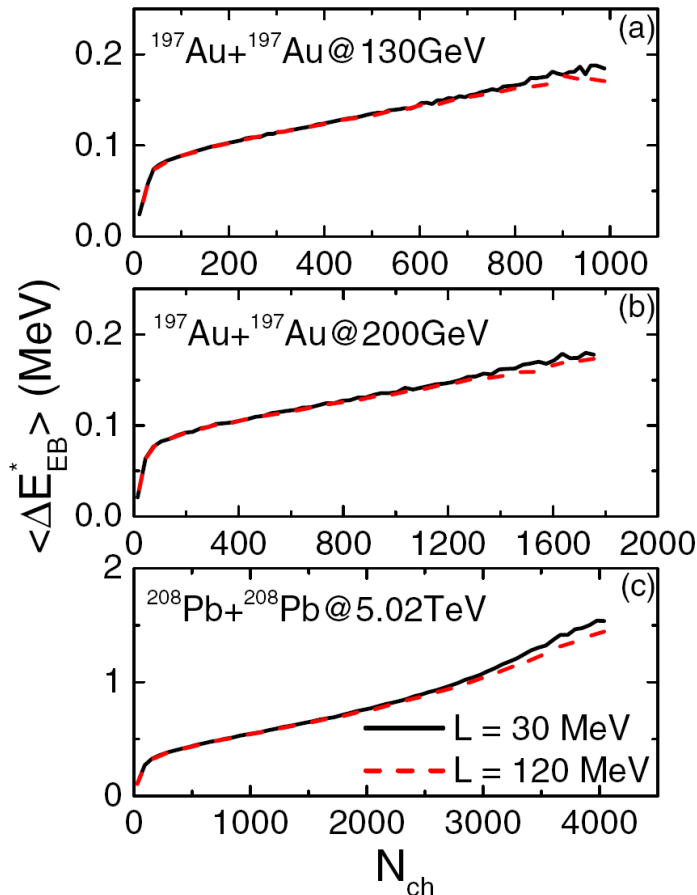
$$e\vec{E}(t, \vec{r}) = \frac{e^2}{4\pi\epsilon_0} \sum_i Z_i \frac{1 - v_i^2}{(R_i - \vec{R}_i \cdot \vec{v}_i)^3} (\vec{R}_i - R_i \vec{v}_i)$$

$$e\vec{B}(t, \vec{r}) = \frac{e^2}{4\pi\epsilon_0} \sum_i Z_i \frac{1 - v_i^2}{(R_i - \vec{R}_i \cdot \vec{v}_i)^3} \vec{v}_i \times \vec{R}_i,$$

Assuming free propagation of nucleons

$$\frac{dp_i^0}{dt} = eZ_i [\vec{E}(t, \vec{r}_i) + \vec{v}_i \times \vec{B}(t, \vec{r}_i)] \cdot \vec{v}_i$$

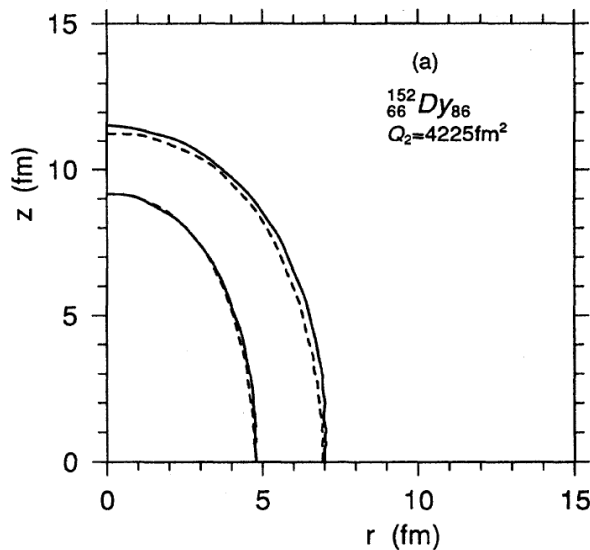
$$\frac{d\vec{p}_i}{dt} = eZ_i [\vec{E}(t, \vec{r}_i) + \vec{v}_i \times \vec{B}(t, \vec{r}_i)].$$



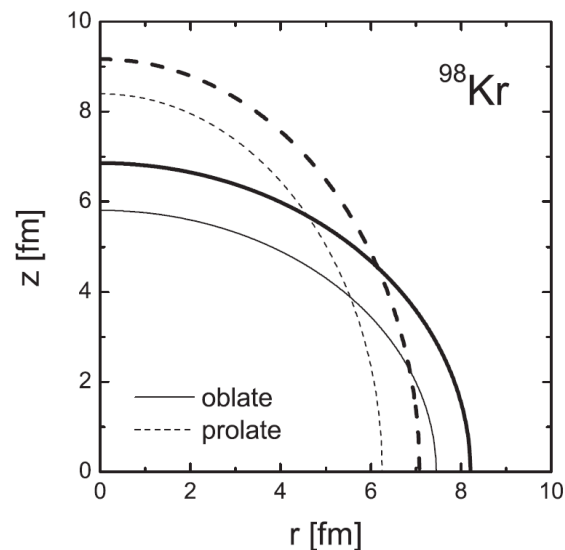
Relevant studies on $\Delta r_{np}(\theta)$ in deformed nuclei

Similar Δr_{np} in r and z directions

SHF+BCS



Different Δr_{np} in r and z directions

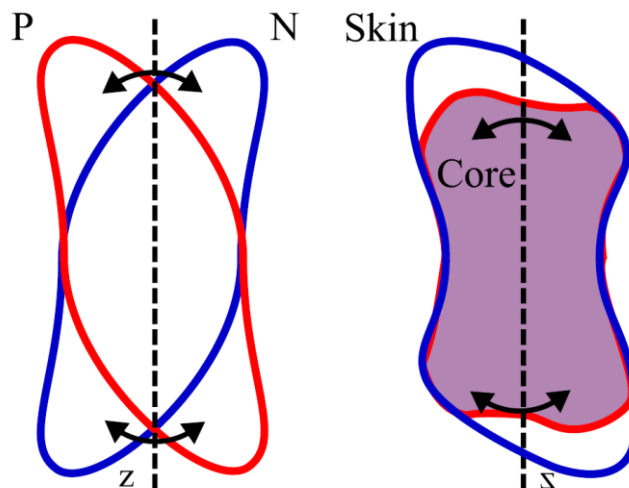


I. Hamamoto and X.Z. Zhang, PRC (1995)

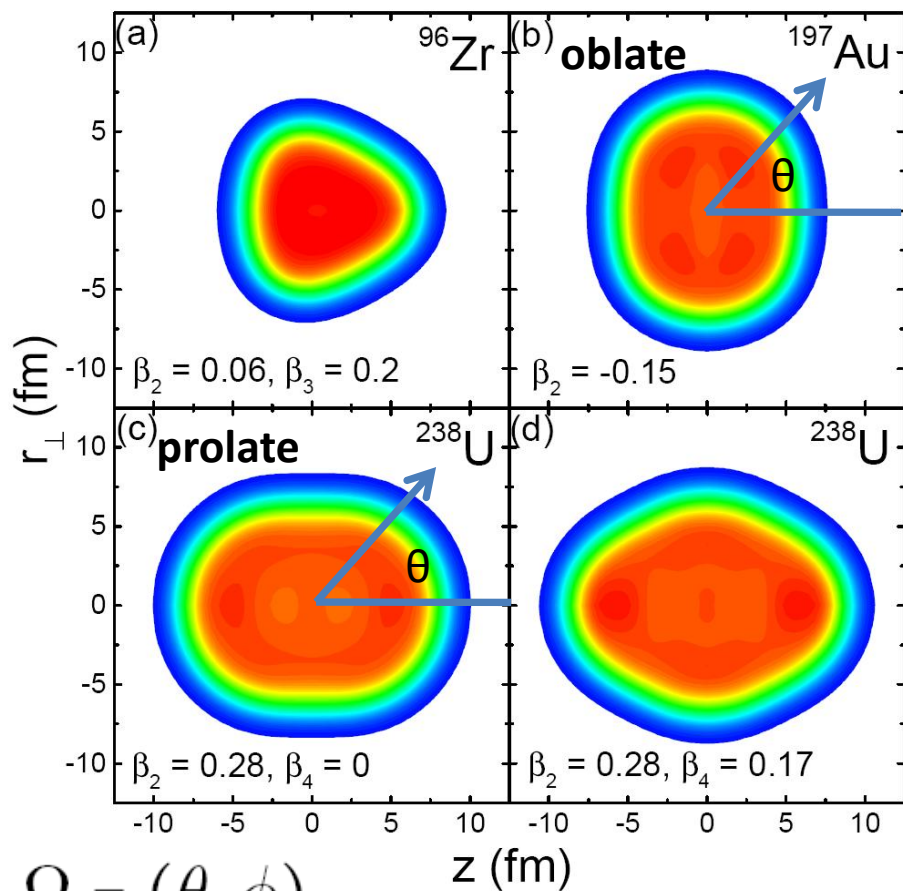
P. Sarriguren et al., PRC (2007)

Affect the scissor-like motion (M1) in deformed nuclei

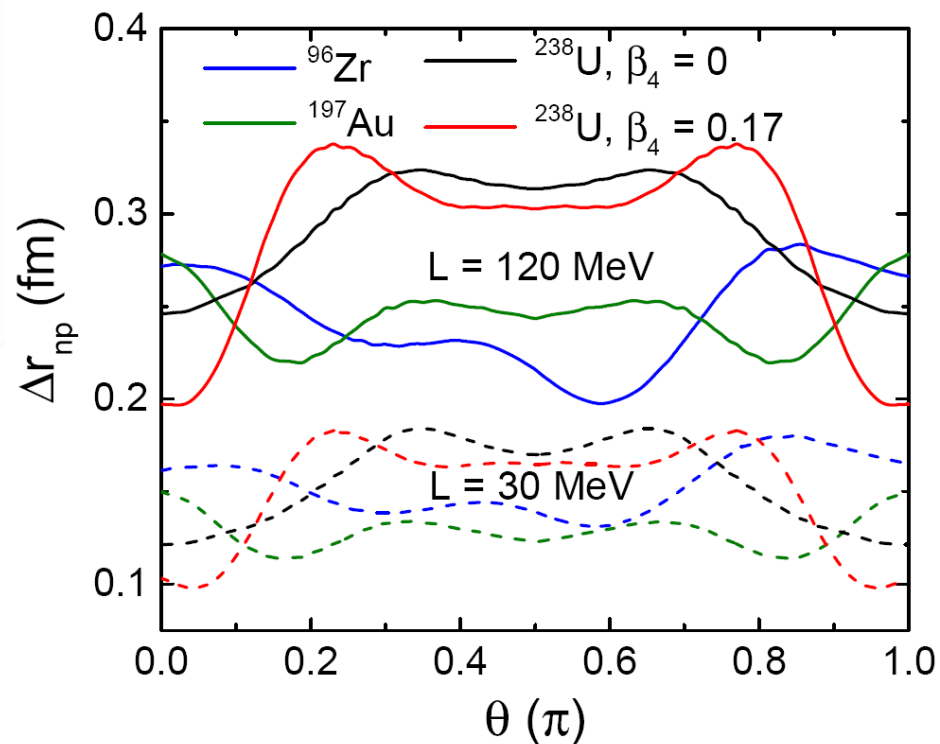
D. Pena Arteaga and P. Ring, arXiv: 0912.0908 [nucl-th]



Δr_{np} effect from different collision configurations



Nucleus	Deformation(s)	$\overline{\Delta r_{np}}$ (fm)	
		$L = 30$ MeV	$L = 120$ MeV
^{96}Zr	$\beta_2=0.06, \beta_3=0.2$ [43]	0.145	0.227
^{197}Au	$\beta_2=-0.15$ [44]	0.127	0.243
^{238}U	$\beta_2=0.28$ [42], $\beta_4=0$	0.156	0.291
	$\beta_2=0.28$ [42], $\beta_4=0.17$	0.153	0.291

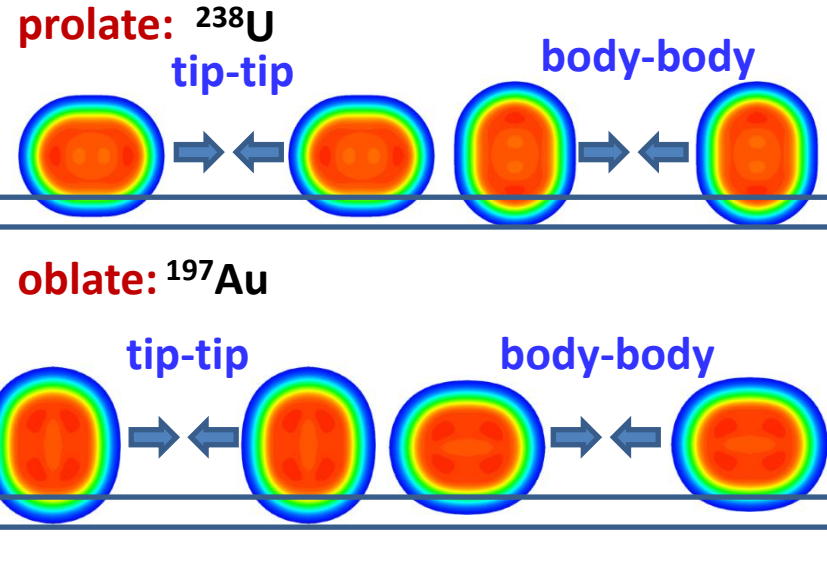
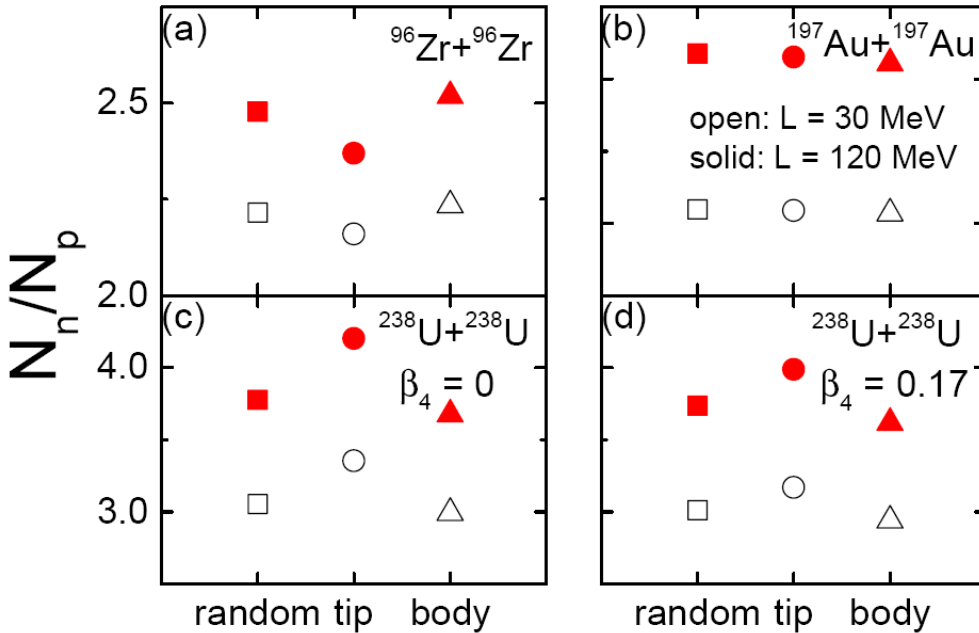


$$\Delta r_{np}(\Omega) = \sqrt{\langle r_n^2(\Omega) \rangle} - \sqrt{\langle r_p^2(\Omega) \rangle}$$

$$\sqrt{\langle r_\tau^2(\Omega) \rangle} = \left(\frac{\int \rho_\tau(r, \Omega) r^4 dr}{\int \rho_\tau(r, \Omega) r^2 dr} \right)^{1/2}$$

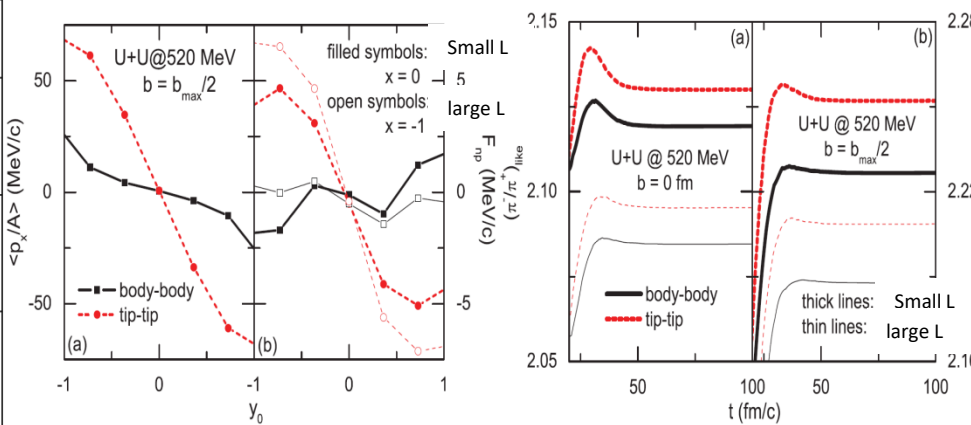
Δr_{np} effect from different collision configurations

$b=0$ fm



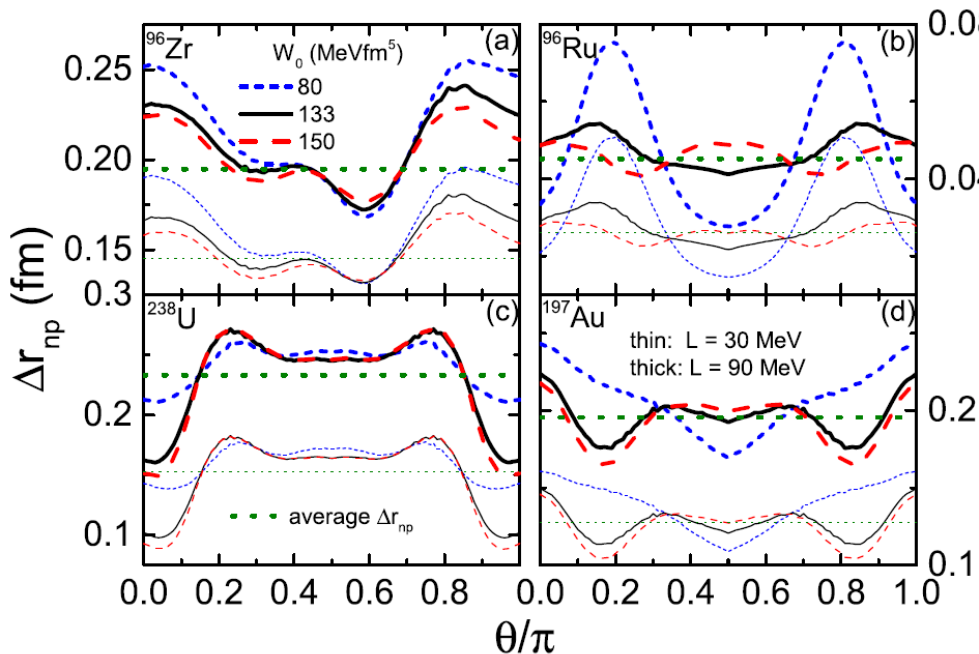
E_{sym} effect from different collision configurations at lower collision energy

	N_n/N_p		$\Delta(N_n/N_p)$
	$L = 30$ MeV	$L = 120$ MeV	
Random			
Tip-tip			
Body-body			
Random			
Tip-tip			
Body-body			
Random			
Tip-tip			
Body-body			
Random			
Tip-tip			
Body-body			



JX, Z. Martinot, and B.A. Li, PRC (2012)

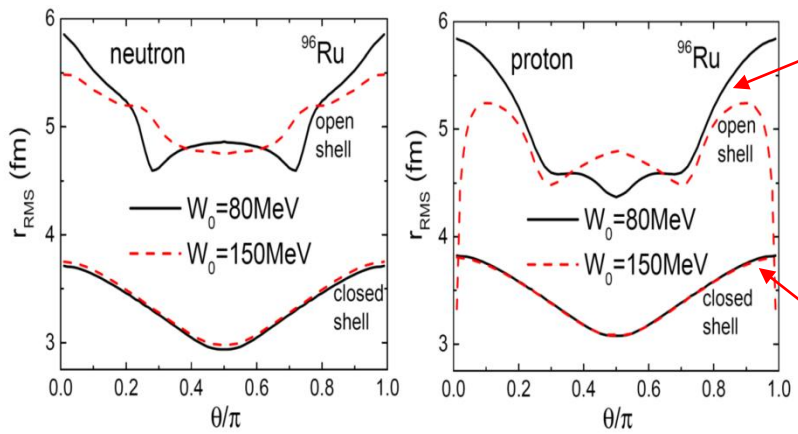
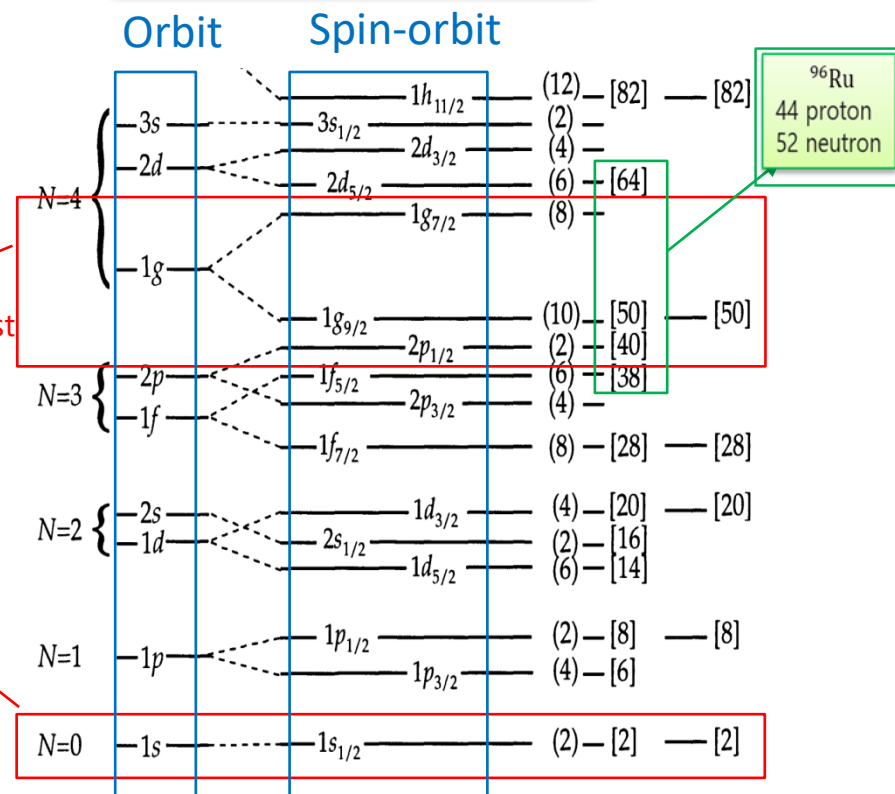
Deformed Δr_{np} from different SO interactions



SO interaction: affect nucleons in open shells for spin unsaturated nuclei, which contribute to the **angular dependence of Δr_{np}**
 $L \sim U_n - U_p$ has a global effect

Spin-orbit interaction (SOI)

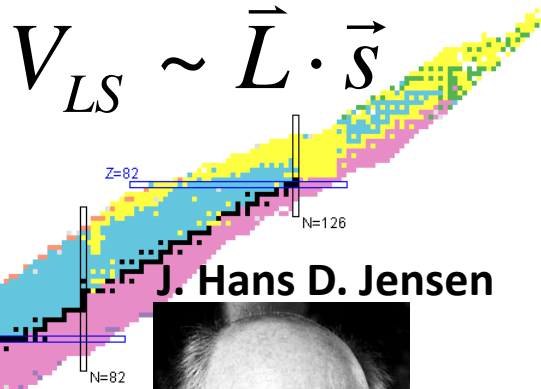
$$v_{so} = iW_0(\vec{\sigma}_1 + \vec{\sigma}_2) \cdot \vec{k}' \times \delta(\vec{r}_1 - \vec{r}_2)\vec{k}$$



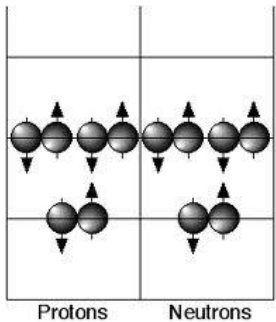
Angular distributions of the RMS radii for typical neutrons (left) and protons (right) in loosely-bound open shells and tightly-bound closed shells of ^{96}Ru using different W_0

Importance of SO interaction

Maria Goeppert Mayer



J. Hans D. Jensen



- **Strength:** $W_0 = 80\sim 150 \text{ MeV fm}^5$
- **Isospin dependence:** kink of Pb isotope charge radii
- **Density dependence:** bubble nuclei

• Skyrme-Hartree-Fock model

$$h_q = \frac{p^2}{2m} + U_q + \vec{W}_q \cdot (\vec{p} \times \vec{\sigma}), (q = n, p)$$

Hartree-Fock method

$$\vec{W}_q = \frac{W_0}{2} (\nabla \rho + \nabla \rho_q)$$

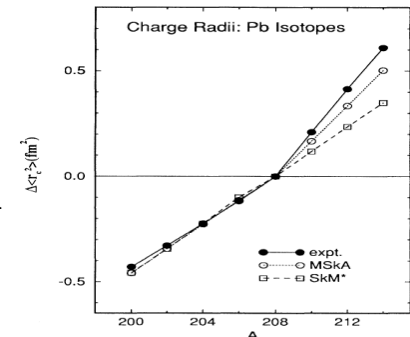
Schrödinger equation: $h_q \varphi_q = e_q \varphi_q$

• Relativistic mean-field model

Dirac equation

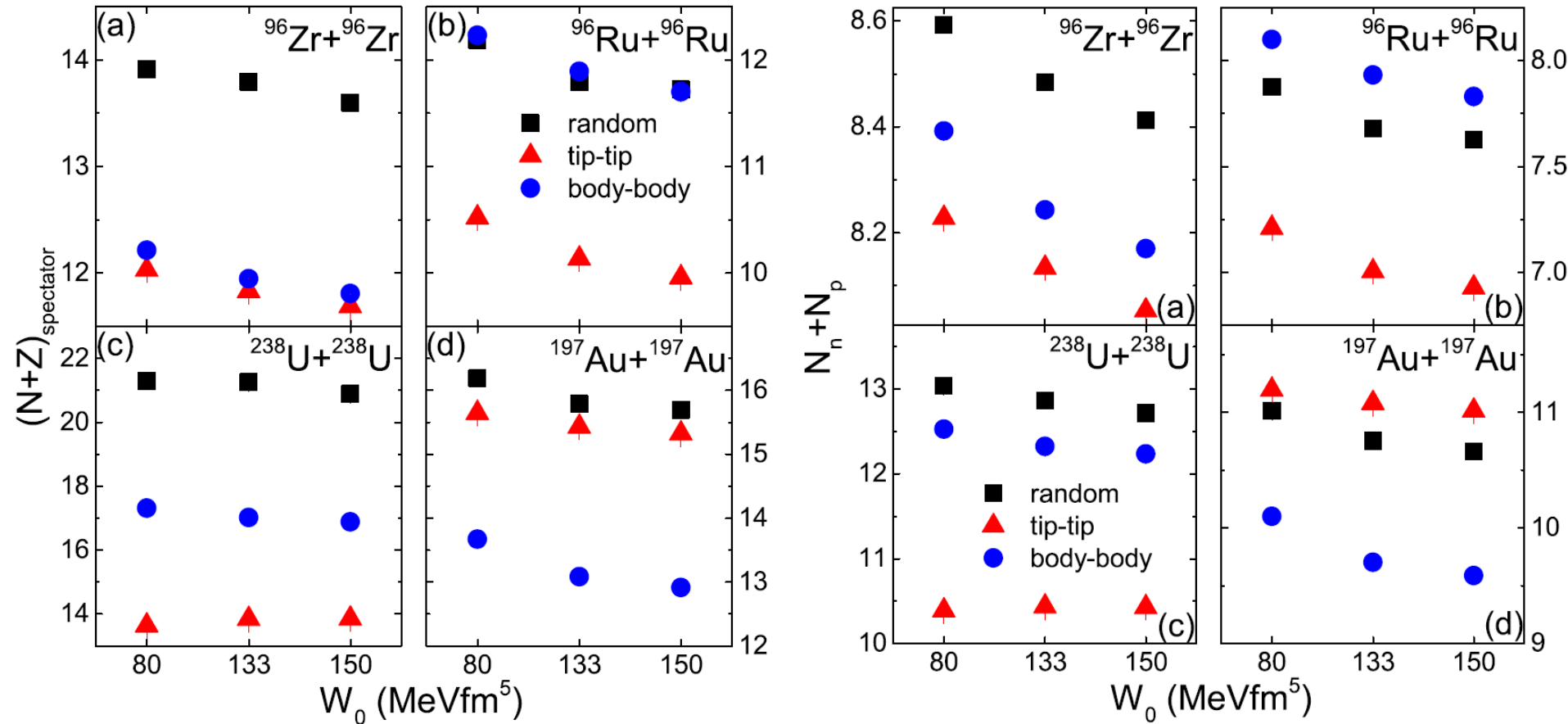
Non-relativistic expansion

$$\vec{W}_q = \frac{C}{(2m - C\rho)^2} \nabla \rho, C = \frac{g_\sigma^2}{m_\sigma^2} + \frac{g_\omega^2}{m_\omega^2}$$



Spectator nucleons from different W_0

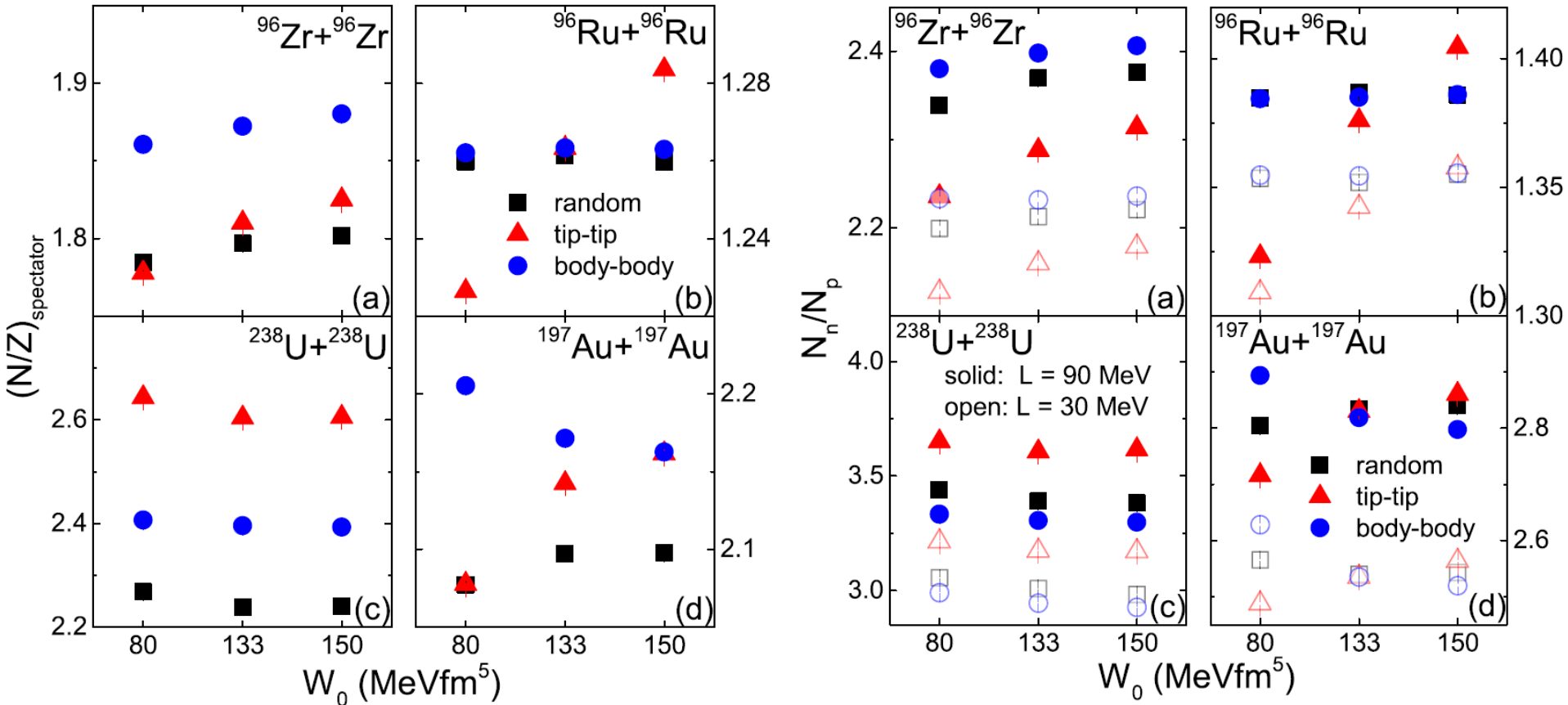
$b=0$ fm



- Collisions with random orientation generally have the largest $(N+Z)_{\text{spectator}}$
- Tip-tip (body-body) collisions by prolate (oblate) nuclei have the smallest $(N+Z)_{\text{spectator}}$
- About 2/3 spectator nucleons become free nucleons

Spectator nucleons from different W_0

$b=0$ fm



- Isospin asymmetry increased for free spectator nucleons compared to spectator matter
- Comparing N_n/N_p in triggered tip-tip and body-body Ru+Ru as well as Au+Au collisions may probe $\Delta r_{np}(\theta)$ and W_0
- Such effect is independent of L

Summary

- Free spectator nucleons N_n, N_p : clean probes
- Ultracentral HIC: free from deexcitations
- Ratio of neutron-rich to neutron-poor system:
 - $(N_n)^{Zr+Zr}/(N_n)^{Ru+Ru}$ reduce uncertainties
 - $(N_n/N_p)^{Zr+Zr}/(N_n/N_p)^{Ru+Ru}$ cancel detecting efficiency
- Triggering collision configurations: measure $\Delta r_{np}(\theta)$

Key question:

**way to unify different/contradictory experimental data
PREXII and CREX, ^{208}Pb nskin and other probes**

Thank you!

junxu@tongji.edu.cn

About anti E_{sym}^0 - L correlation from Nskin

We illustrate the idea with a popularly used symmetry energy of the following form,

$$E_{\text{sym}}(\rho) = E_{\text{sym}}^0 \left(\frac{\rho}{\rho_0} \right)^\gamma. \quad (\text{A1})$$

Thus, the slope parameter L of the symmetry energy can be expressed as

$$L = 3\rho_0 \left[\frac{dE_{\text{sym}}(\rho)}{d\rho} \right]_{\rho_0} = 3E_{\text{sym}}^0 \gamma. \quad (\text{A2})$$

For a fixed symmetry energy at a subsaturation density ρ^* ,

$$E_{\text{sym}}(\rho^*) = E_{\text{sym}}^0 \left(\frac{\rho^*}{\rho_0} \right)^\gamma, \quad (\text{A3})$$

the expression of L in terms of E_{sym}^0 is

$$L = 3E_{\text{sym}}(\rho^*) \left[\frac{E_{\text{sym}}^0}{E_{\text{sym}}(\rho^*)} \right] \frac{\ln[E_{\text{sym}}^0/E_{\text{sym}}(\rho^*)]}{\ln(\rho_0/\rho^*)}. \quad (\text{A4})$$

It is obviously seen that L increases with increasing E_{sym}^0 (see Ref. [64] as an example). The slope parameter at ρ^* can be expressed as

$$L(\rho^*) = 3\rho^* \left[\frac{dE_{\text{sym}}(\rho)}{d\rho} \right]_{\rho^*} = L \left(\frac{\rho^*}{\rho_0} \right)^\gamma, \quad (\text{A5})$$

where $L(\rho^*)$ is seen to be smaller than L . For a fixed $L(\rho^*)$, the expression of E_{sym}^0 in terms of L is

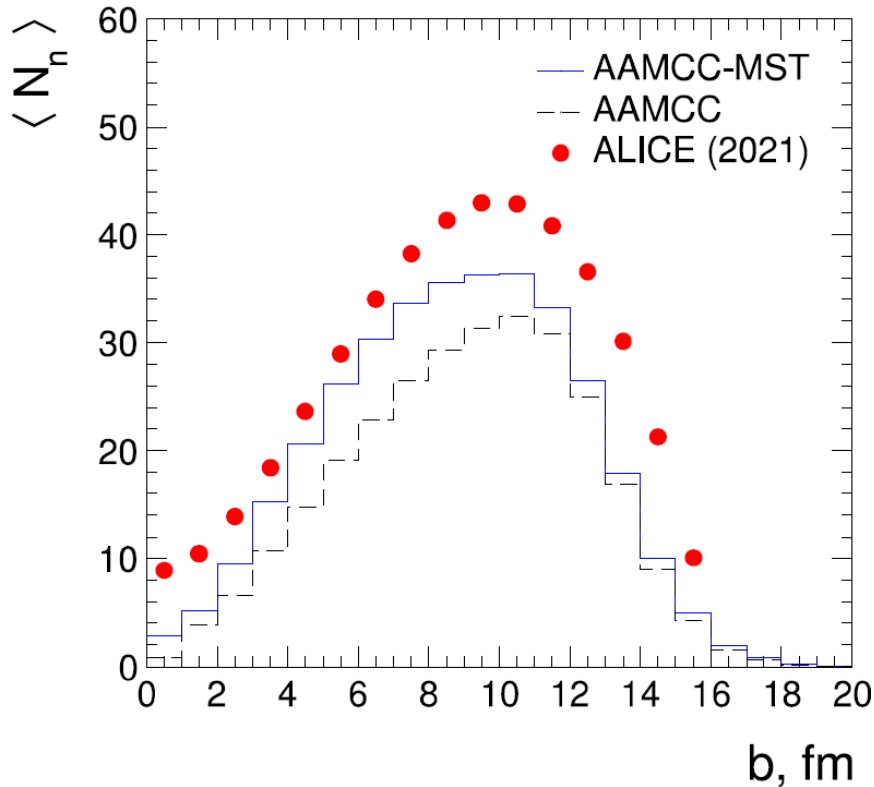
$$E_{\text{sym}}^0 = \frac{L(\rho^*)}{3} \frac{\ln(\rho^*/\rho_0)}{[L(\rho^*)/L] \ln[L(\rho^*)/L]}. \quad (\text{A6})$$

The function $x \ln(x)$ is negative for $x < 1$ and increases with increasing x for $x > 0.4$. Thus, E_{sym}^0 generally increases with increasing $x = L(\rho^*)/L$. Because L decreases with increasing x , this leads to an anticorrelation between L and E_{sym}^0 . This conclusion is general and helps us understand the results shown in Fig. 2 of the present manuscript.

JX, W.J. Xie, and B.A. Li, PRC (2020)

Results and discussions: ZDC background

$^{208}\text{Pb}+^{208}\text{Pb}@5.02\text{TeV}$



R. Nepeivoda et al., Particles (2022)

A+B String-melting AMPT

